Supporting Information (SI) Appendix

Design and characterization of synthetic fungal-bacterial consortia for direct production of isobutanol from cellulosic biomass

Jeremy J. Minty[1], Marc E. Singer[1], Scott A. Scholz[2], Chang-Hoon Bae[1], Jung-Ho Ahn[1], Clifton E. Foster[3], James C. Liao[4], and Xiaoxia Nina Lin[1]

[1]Chemical Engineering, University of Michigan, Ann Arbor, MI
[2]Cellular and Molecular Biology Ph.D. Program, University of Michigan, Ann Arbor, MI
[3]Great Lakes Bioenergy Research Center, Michigan State University, Lansing, MI
[4]Chemical and Biomolecular Engineering, University of California, Los Angeles, CA

Contents

List of Figures

List of Tables

1 TrEc model

1.1 Introduction

To gain insights into the behavior and ecology of the *T. reesei* / *E. coli* (TrEc) consortium, we developed a comprehensive ordinary differential equation (ODE) modeling framework that captures salient features of the system. We derived rate expressions for microbial growth, uptake of soluble saccharides, production of cellulase enzymes (endoglucanase, exoglucanase, and β-glucosidase) by *T. reesei*, enzymatic cellulose hydrolysis (based on novel mechanistic models for each type of enzyme), isobutanol production by *E. coli*, and isobutanol toxicity. The model was developed by writing differential mole/mass balances (for a batch reactor) for each species of interest, including microbial biomass (*T. reesei* and *E. coli*), cellulases, insoluble cellulose polysaccharides, soluble oligo and monosaccharides, and isobutanol. We give a comprehensive description of our framework in the following sections. We provide detailed derivations for our novel substrate uptake and enzymatic cellulose hydrolysis kinetics, and for our mass transfer model of *T. reesei* privileged access to soluble saccharides.

1.2 Microbial growth and substrate utilization

1.2.1 Maintenance model

Substrate consumption by microbes has two components: substrate consumed for growth, and substrate consumed for non-growth associated maintenance. We expect that maintenance substrate consumption will be important in the *T. reesei* / *E. coli* consortium due to low growth rates. Maintenance substrate uptake is usually empirically modeled as follows [1]:

$$r_{sm} = mC_c \tag{S1}$$

where r_{sm} is maintenance substrate uptake rate (g/L/h), m is the maintenance coefficient (g-substrate/g-cells/h), and C_c is cell concentration (g/L). We find this model to be unrealistic, however, as it supposes that substrate uptake rate is completely independent of substrate concentration. This assumption may be reasonable in situations involving high substrate concentrations (e.g. batch culture growth on soluble substrates), but for growth on cellulosic substrates,

concentrations of soluble saccharides are likely to be very low, requiring us to consider the actual kinetics of substrate uptake. We thus propose an alternative maintenance model centered on substrate uptake kinetics. We assume that total substrate uptake follows Michaelis-Menten kinetics, and allow for the uptake of multiple substrates simultaneously [2]. Uptake rate of substrate S_i can then be modeled as:

$$r_{S_i} = p_{S_i} \frac{K_{max,S_i} S_i}{K_{S_i} + S_i} C_c \text{ with } p_{S_i} = \frac{S_i}{\sum_j S_j} \tag{S2}$$

where r_{S_i} is uptake rate of substrate i (g/L/h), p_{S_i} is the fraction of substrate i out of total soluble substrate, K_{max,S_i} is maximum specific uptake rate of substrate i (g-substrate/g-cells/h), K_{S_i} is affinity for substrate i (g/L), S_i is concentration of substrate i (g/L), and C_c is cell concentration (g/L). We assume that substrate is partitioned between growth and maintenance uses. We can thus write a mass balance for substrate uptake as follows:

$$r_{S_i} = p_{S_i} \frac{K_{max,S_i} S_i}{K_{S_i} + S_i} C_c = Y_{S_i/C_c} \mu_{S_i} C_c + m p_{S_i} C_c \tag{S3}$$

where Y_{S_i/C_c} is the substrate-biomass yield coefficient (g-substrate/g-cells), μ_{S_i} is specific growth rate on substrate i (1/h), and other terms are as described previously. The term $Y_{S_i/C_c} \mu_{S_i} C_c$ represents substrate consumption for growth, while the $m p_{S_i} C_c$ term represents maintenance consumption. If we hold m constant (i.e. assume constant maintenance requirement), then we can rearrange and write μ_{S_i} in terms of the other parameters and variables:

$$\mu_{S_i} = \frac{p_{S_i}}{Y_{S_i/C_c}} \left(\frac{K_{max,S_i} S_i}{K_{S_i} + S_i} - m \right) \tag{S4}$$

The maximum specific growth rate $\mu_{S_i,max}$ corresponds to $S_i \gg K_{S_i}$ with i as the sole substrate:

$$\mu_{S_i,max} = \frac{1}{Y_{S_i/C_c}} \left(K_{max,S_i} - m \right) \tag{S5}$$

Since $\mu_{S_i,max}$ is readily available from experimental data, it makes sense to reformulate our model in terms of this parameter:

$$K_{max,S_i} = Y_{S_i/C_c} \mu_{S_i,max} + m \tag{S6}$$

Microbial growth rate can then be written as:

$$r_{g,S_i} = \mu_{S_i} C_c = p_{S_i} \left[\left(\mu_{S_i,max} + \frac{m}{Y_{S_i/C_c}} \right) \frac{S_i}{K_{S_i} + S_i} - \frac{m}{Y_{S_i/C_c}} \right] C_c \tag{S7}$$

where r_{g,S_i} is growth rate on substrate i (g/L/h) and all other terms are as described previously. Substrate consumption can be written as:

$$r_{S_i} = p_{S_i} \frac{K_{max,S_i} S_i}{K_{S_i} + S_i} C_c = p_{S_i} \left(Y_{S_i/C_c} \mu_{S_i,max} + m \right) \frac{S_i}{K_{S_i} + S_i} C_c \tag{S8}$$

We can write the total growth rate as:

$$r_g = \sum_i r_{g,S_i} = \sum_i \left[p_{S_i} \left(\left(\mu_{S_i,max} + \frac{m}{Y_{S_i/C_c}} \right) \frac{S_i}{K_{S_i} + S_i} - \frac{m}{Y_{S_i/C_c}} \right) C_c \right] \tag{S9}$$

where all terms are as described previously.

1.2.2 *T. reesei* privileged access to substrate

Accounting for the hydrolysis of cellulosic feedstocks to soluble bioavailable saccharides is a crucial aspect of modeling the *T. reesei* / *E. coli* consortium. An important subtlety in this process is that soluble oligosaccharides (i.e. saccharides 2 to 4 glucose monomers in size) are hydrolyzed to glucose via β-glucosidase bound to the cell wall of *T. reesei* [3], as depicted in Fig S1A. This leads to locally increased concentration of glucose at the cell surface relative to the bulk media, thus affording privileged access to *T. reesei*. We perform a mass-transfer analysis to estimate the concentration of glucose at the cell surface, making the following assumptions:

1. Soluble oligosaccharides are hydrolyzed by β-glucosidase via a heterogenous Michaelis-Menten reaction at the cell surface.

2. Concentration of soluble saccharides is lower than β-glucosidase affinity ($S_{G_i} < K_{M,G_i}^{BGL}$) — reasonable for co-culture conditions.

3. No homogenous hydrolysis reactions in the bulk media.

4. Pseudo steady state conditions — reasonable due to large timescale for changes in bulk saccharide concentrations.

5. Most of the glucose produced at the *T. reesei* cell surface is lost to diffusion (verified in [4] for *S. cerevisiae* / sucrose hydrolysis).

6. The cell surface is surrounded by a stagnant boundary layer of depth δ which provides the primary resistance to mass transfer to the bulk media (Fig S1B).

7. *T. reesei* mycelial geometry can be approximated as cylindrical (Fig S1B).

Based on assumption 2, we can simplify β-glucosidase kinetics to yield the following rate law for hydrolysis of soluble saccharides:

$$r_{S_{G_i}}^{BGL} \approx -\frac{k_{cat,BGL,G_i}\rho_E}{K_{M,G_i}^{BGL}} S_{G_i} = -k_{BGL,G_i} S_{G_i} \tag{S10}$$

$$k_{BGL,G_i} = \frac{k_{cat,BGL,G_i}\rho_E}{K_{M,G_i}^{BGL}} \tag{S11}$$

where $r_{S_{G_i}}^{BGL}$ is the cellobiose hydrolysis rate per unit area (mmol/dm^2/h), k_{cat,BGL,G_i} is the specific activity of β-glucosidase for substrate i (mmol/g-BGL/h), ρ_E is the density of β-glucosidase on the cell surface (g-BGL/dm^2), K_{M,G_i}^{BGL} is affinity of β-glucosidase for substrate i (mM), S_{G_i} is concentration of substrate i (mM; i is equivalent to degree of polymerization DP, i.e. number of glucose monomers), and k_{BGL,G_i} is an apparent first-order rate constant (dm/h). Applying conservation equations and simplifying yields the following:

$$\nabla \cdot N_{G_i} = 0 \tag{S12}$$

$$\nabla^2 S_{G_i} = 0 \tag{S13}$$

where N_{G_i} is the molar flux of substrate i (mmol/dm^2/h) and other terms are as defined previously. By argument of symmetry (Fig S1B) we can neglect all components except for the radial direction, allowing us to simply further:

$$\frac{1}{r}\frac{d}{dr}\left(r\frac{dS_{G_i}}{dr}\right) = 0 \tag{S14}$$

The above equation can be solved to yield a concentration profile of S_{G_i} as a function of position by applying the following boundary conditions:

$$S_{G_i} = S_{G_i,0} \text{ at } r = R + \delta \tag{S15}$$

$$S_{G_i} = S_{G_i,Tr} \text{ at } r = R \tag{S16}$$

where $S_{G_i,0}$ is the bulk concentration of substrate i (mM), $S_{G_i,Tr}$ is the concentration of substrate i at the *T. reesei* mycelium surface (mM), R is the hyphal radius (dm), and δ is the boundary layer thickness (dm). Integrating and applying the above BCs yields:

$$S_{G_i} = (S_{G_i,Tr} - S_{G_i,0})\frac{\ln r - \ln(R+\delta)}{\ln R - \ln(R+\delta)} + S_{G_i,0} \tag{S17}$$

Next we apply a mole balance to the interface between the boundary layer and the mycelium surface, equating the diffusive flux at the surface to the rates of hydrolysis of substrate i and production of substrate i from hydrolysis of $i+1$ saccharides:

$$-D_{G_i}\frac{dS_{G_i}}{dr}\bigg|_{r=R} = r^{BGL}_{S_{G_i}} - r^{BGL}_{S_{G_{i+1}}} = -k_{BGL,G_i}S_{G_i,Tr} + k_{BGL,G_{i+1}}S_{G_{i+1},Tr} \tag{S18}$$

where D_{G_i} is the diffusion coefficient of substrate i (dm^2/h), $-D_{G_i}\frac{dS_{G_i}}{dr}$ is the diffusive flux of substrate i (mmol/dm^2/h), $r^{BGL}_{S_{G_i}}$ is the hydrolysis rate of substrate i on the mycelium surface (mmol/dm^2/h), and $r^{BGL}_{S_{G_{i+1}}}$ is the hydrolysis rate of substrate $i+1$ at the mycelium surface (mmol/dm^2/h). Substituting the radial concentration profile S_{G_i} in the derivative above and rearranging yields the following expression for $S_{G_i,Tr}$:

$$S_{G_i,Tr} = \frac{R\ln\left(\frac{R}{R+\delta}\right)}{-D_{G_i}}\left[-k_{BGL,G_i}S_{G_i,Tr} + k_{BGL,G_{i+1}}S_{G_{i+1},Tr}\right] + S_{G_i,0} \tag{S19}$$

To estimate a value for δ, we can assume that the stagnant boundary layer is the primary barrier to mass transfer. The mass transfer coefficient is then simply given by Sherwood number $Sh = 2.0$ and therefore $\delta \approx R$. The above equation then simplifies to:

$$S_{G_i,Tr} = \frac{-k_{BGL,G_i}S_{G_i,Tr} + k_{BGL,G_{i+1}}S_{G_{i+1},Tr}}{D_{G_i}}R\ln 2 + S_{G_i,0} \tag{S20}$$

We calculate the surface concentrations of each soluble saccharide (DP=1 to 4) as follows:

Cellotetraose: DP=4

$$S_{G_4,Tr} = \frac{-k_{BGL,G_4}S_{G_4,Tr}}{D_{G_4}}R\ln 2 + S_{G_4,0} \tag{S21}$$

Rearranging,

$$\frac{S_{G_4,Tr}}{S_{G_4,0}} = \frac{1}{1+\frac{k_{BGL,G_4}R\ln 2}{D_{G_4}}} = \eta_4 \tag{S22}$$

with parameters defined for substrate i as:

$$\eta_i = \frac{1}{1+k_{BGL,G_i}\phi_i} \tag{S23}$$

$$\phi_i = \frac{R\ln 2}{D_{G_i}} \tag{S24}$$

where η_i is the ratio of mycelium surface concentration to bulk concentration for substrate i, and ϕ_i is the ratio of characteristic boundary layer length to the diffusion coefficient for substrate i (h/dm)

Cellotriose: DP=3

$$S_{G_3,Tr} = \frac{-k_{BGL,G_3}S_{G_3,Tr} + k_{BGL,G_4}S_{G_4,Tr}}{D_{G_3}}R\ln 2 + S_{G_3,0} \tag{S25}$$

which can be rearranged to yield:

$$S_{G_3,Tr} = k_{BGL,G_4}\phi_3\eta_3 S_{G_4,Tr} + \eta_3 S_{G_3,0} \tag{S26}$$

$$= k_{BGL,G_4}\phi_3\eta_3\eta_4 S_{G_4,0} + \eta_3 S_{G_3,0} \tag{S27}$$

with parameters defined as above.

Cellobiose: DP=2 Proceeding as for cellotetraose and cellotriose:

$$S_{G_2,Tr} = k_{BGL,G_3}\phi_2\eta_2 S_{G_3,Tr} + \eta_2 S_{G_2,0} \tag{S28}$$

$$= \frac{-k_{BGL,G_2}S_{G_2,Tr} + k_{BGL,G_3}S_{G_3,Tr}}{D_{G_2}}\left(R\ln 2\right) + S_{G_2,0} \tag{S29}$$

$$= k_{BGL,G_3}\phi_2\eta_2\left(k_{BGL,G_4}\phi_3\eta_3\eta_4 S_{G_4,0} + \eta_3 S_{G_3,0}\right) + \eta_2 S_{G_2,0} \tag{S30}$$

with parameters defined as above.

Glucose For glucose, we modify the interfacial mole balance since glucose is the product of all β-glucosidase hydrolysis reactions:

$$-D_{G_1}\left.\frac{dS_{G_1}}{dr}\right|_{r=R} = 2r_{S_{G_2}}^{BGL} + r_{S_{G_3}}^{BGL} + r_{S_{G_4}}^{BGL} \tag{S31}$$

$$= -2k_{BGL,G_2}S_{G_2,Tr} - k_{BGL,G_3}S_{G_3,Tr} - k_{BGL,G_4}S_{G_4,Tr} \tag{S32}$$

where all terms are as defined previously. Proceeding as above, $S_{G_1,Tr}$ can be expressed as:

$$S_{G_1,Tr} = \left(2k_{BGL,G_2}S_{G_2,Tr} + k_{BGL,G_3}S_{G_3,Tr} + k_{BGL,G_4}S_{G_4,Tr}\right)\phi_1 + S_{G_1,0} \tag{S33}$$

which can be simplified to the following expression by substituting in the above expressions for $S_{G_2,Tr}$, $S_{G_3,Tr}$, and $S_{G_4,Tr}$ and making some rearrangements:

$$S_{G_1,Tr} = S_{G_1,0} + \theta_2 S_{G_2,0} + \theta_3 S_{G_3,0} + \theta_4 S_{G_4,0} \tag{S34}$$

where the θ coefficients are recursively defined as follows:

$$\theta_2 = \frac{2k_{BGL,G_2}\phi_1}{1 + k_{BGL,G_2}\phi_2} \tag{S35}$$

$$\theta_3 = \theta_2\frac{k_{BGL,G_3}\phi_2}{1 + k_{BGL,G_3}\phi_3} + \frac{k_{BGL,G_3}\phi_1}{1 + k_{BGL,G_3}\phi_3} = \left(\theta_2\phi_2 + \phi_1\right)\frac{k_{BGL,G_3}}{1 + k_{BGL,G_3}\phi_3} \tag{S36}$$

$$\theta_4 = \left(\theta_3\phi_3 + \phi_1\right)\frac{k_{BGL,G_4}}{1 + k_{BGL,G_4}\phi_4} \tag{S37}$$

$$\tag{S38}$$

Proposed general framework In general, we can describe the surface concentration of any soluble saccharide in terms of coefficients similar to those defined above for glucose. A proposed framework:

$$S_{G_i,Tr} = S_{G_i,0} + \sum_{k=i+1}^{4}\theta_{k\to i}S_{G_k,0} \tag{S39}$$

where $\theta_{k\to i}$ is the contribution of substrate i concentration at the mycelium surface due to hydrolysis of substrate k (mM/mM or any other ratio of consistent concentration units)

1.3 *T. reesei* model

1.3.1 *T. reesei* growth

T. reesei is a multicellular filamentous fungus that has different mycelial growth states. Vegetative growth and enzyme secretion are highly active at hyphal tips, while senescent mycelium is relatively dormant [5]. Assuming that growth at hyphal tips follows Monod kinetics and that *T. reesei* is capable of simultaneous utilization of multiple soluble sugars

(i.e. glucose and soluble glucose oligosaccharides), *T. reesei* growth in the presence of isobutanol can be described with a segregated kinetic model:

$$\frac{dC_{Tr,v}}{dt} = \mu_{Tr} C_{Tr,v} - k_{v\to s} C_{Tr,v} \tag{S40}$$

$$\frac{dC_{Tr,s}}{dt} = k_{v\to s} C_{Tr,v} - k_{Tr,d} C_{Tr,s} \tag{S41}$$

In the first expression, $C_{Tr,v}$ is the vegetative mycelium concentration (g/L), μ_{Tr} is a generalized Monod function (1/h) depending on isobutanol concentration I (g/L) and concentration of soluble glucose saccharides S_{G_i} (g/L; i is the degree of polymerization), and $k_{v\to s}$ is the specific rate of conversion of vegetative mycelium to senescent mycelium (1/h). In the second expression, $C_{Tr,s}$ is the concentration of senescent mycelium (g/L) and $k_{Tr,d}$ is the specific death rate of senescent mycelium (1/h). We formulate μ_{Tr} as follows:

$$K_{Tr}^{I} = \begin{cases} \left(1 - \frac{I}{I_{Tr}^{*}}\right)^{n_{Tr}} & \text{if } I \le I_{Tr}^{*} \\ 0 & \text{if } I > I_{Tr}^{*} \end{cases} \tag{S42}$$

$$\mu_{Tr} = K_{Tr}^{I} \sum_{i} p_{S_{G_i}} \left[\left(\mu_{max,Tr,S_{G_i}} + \frac{m_{Tr}}{Y_{S_{G_i}/C_{Tr}}} \right) \frac{S_{G_i} + \sum_{k=i+1}^{4} \theta_{k\to i} S_{G_k}}{K_{Tr,S_{G_i}} + S_{G_i} + \sum_{k=i+1}^{4} \theta_{k\to i} S_{G_k}} - \frac{m_{Tr}}{Y_{S_{G_i}/C_{Tr}}} \right] \tag{S43}$$

$$\text{with } p_{S_{G_i}} = \frac{S_{G_i}}{\sum_{j} S_{G_j}}$$

where K_{Tr}^{I} is an empirical inhibition function (dimensionless) [1], I is isobutanol concentration (g/L), I_{Tr}^{*} is the growth inhibiting concentration of isobutanol (g/L) for *T. reesei*, n_{Tr} is an empirically determined exponent, $\mu_{max,Tr,S_{G_i}}$ is maximum specific growth rate on substrate i (1/h), $p_{S_{G_i}}$ is the proportion of substrate i in the total substrate concentration ($S_{G_i}/\sum S_{G_k}$), S_{G_i} is substrate i concentration (g/L), $K_{Tr,S_{G_i}}$ is substrate i affinity (g/L), the coefficients $\theta_{k\to i}$ are as described in section 1.2.2, m_{Tr} is the maintenance coefficient (g-substrate/g-biomass/h), and $Y_{S_{G_i}/C_{Tr}}$ is the substrate/biomass yield coefficient for substrate i (g-substrate/g-biomass). We assume that growth occurs via utilization of multiple substrates simultaneously, as opposed to diauxic substrate utilization. Available experimental data suggests that this is a reasonable assumption for *T. reesei*, especially the RUTC30 strain, which contains a loss-of-function mutation in catabolite repression gene *cre1* [6]. Our model assumes a total substrate maintenance requirement m_{Tr} rather than an individual maintenance term for each substrate i; this is reasonable for substrates with similar metabolism / energy yields (e.g. glucose and cellobiose), but could be revised for more diverse substrates.

1.3.2 *T. reesei* enzyme secretion

Assuming that enzyme secretion is stoichiometrically coupled to growth and that composition of secreted enzymes is constant, the following expression can be derived for cellulase production:

$$\frac{dE_T}{dt} = Y_{E_T/C_{Tr}} \mu_{Tr} C_{Tr,v} + k_{E_T} C_{Tr,s} \tag{S44}$$

$$\frac{dE_i}{dt} = x_{E_i} \frac{dE_T}{dt} = x_{E_i} \left[Y_{E_T/C_{Tr}} \mu_{Tr} C_{Tr,v} + k_{E_T} C_{Tr,s} \right] \tag{S45}$$

where E_T is the total concentration of secreted enzymes (g/L), $Y_{E_T/C_{Tr}}$ is the enzyme/biomass yield coefficient (g-protein/g-biomass), k_{E_T} is the specific enzyme production rate of senescent mycelium (g-protein/g-biomass/h), E_i is concentration of enzyme i (g/L), x_{E_i} is the fraction of enzyme i in the total secretome (E_i/E_T), and the other terms are as described in previous sections. *T. reesei* produces a large suite of biomass degrading enzymes, but for the purpose of our cellulose hydrolysis model, we consider the most important enzymes [7]:

- cellobiohydrolase 1 ($CBH1$) and 2 ($CBH2$)

- endoglucanase 1 ($EG1$)
- β-glucosidase 1 (BGL)

1.3.3 *T. reesei* RUTC30 saccharide uptake

Assuming that saccharide uptake is stoichiometrically coupled to growth of vegetative mycelium and that both vegetative and senescent mycelia consume saccharides for maintenance, the following expression for saccharide uptake by *T. reesei* can be derived:

$$r_{S_{G_i}}^{Tr} = \left[Y_{S_{G_i}/C_{Tr}} K_{Tr}^{I} p_{S_{G_i}} \mu_{max,Tr,S_{G_i}} + m_{Tr}\right] \frac{S_{G_i}}{K_{Tr,S_{G_i}} + S_i} C_{Tr,v} + m_{Tr} p_{S_{G_i}} \frac{S_{G_i}}{K_{Tr,S_{G_i}} + S_{G_i}} C_{Tr,s} \quad \text{(S46)}$$

where $r_{S_{G_i}}^{Tr}$ is the total rate of saccharide i uptake by *T. reesei* (g/L/h), and all other terms are as described in previous sections.

1.4 *E. coli* model

1.4.1 *E. coli* growth

We model *E. coli* growth with Monod kinetics [1], assuming that only glucose is utilized for growth (i.e. glucose oligosaccharides cannot be metabolized):

$$\frac{dC_{Ec}}{dt} = \left(\mu_{Ec} - k_{Ec,d}\right) C_{Ec} \quad \text{(S47)}$$

where C_{Ec} is *E. coli* concentration (g/L), μ_{Ec} is specific growth rate (1/h), and $k_{Ec,d}$ is the specific cell death rate (1/h). μ_{Ec} is assumed to be a function of glucose concentration S_{G_1}, with concentration-dependent inhibition from isobutanol:

$$K_{Ec,S_{G_1}}^{I} = \begin{cases} \left(1 - \frac{I}{I_{Ec,S_{G_1}}^{*}}\right)^{n_{Ec,S_{G_1}}} & \text{if } I \leq I_{Ec,S_{G_1}}^{*} \\ 0 & \text{if } I > I_{Ec,S_{G_1}}^{*} \end{cases} \quad \text{(S48)}$$

$$\mu_{Ec} = K_{Ec,S_{G_1}}^{I} \left[\left(\mu_{max,Ec,S_{G_1}} + \frac{m_{Ec,S_{G_1}}}{Y_{S_{G_1}/C_{Ec}}}\right) \frac{S_{G_1}}{K_{Ec,S_{G_1}} + S_{G_1}} - \frac{m_{Ec,S_{G_1}}}{Y_{S_{G_1}/C_{Ec}}}\right] \quad \text{(S49)}$$

where $K_{Ec,S_{G_1}}^{I}$ is an empirical inhibition function (dimensionless) [1], I is isobutanol concentration (g/L), $I_{Ec,S_{G_1}}^{*}$ is the growth inhibiting concentration of isobutanol (g/L) for *E. coli*, $n_{Ec,S_{G_1}}$ is an empirically determined exponent, $\mu_{max,Ec,S_{G_1}}$ is maximum specific growth rate of *E. coli* on glucose (1/h), $K_{Ec,S_{G_1}}$ is glucose affinity (g/L), $Y_{S_{G_1}/C_{Ec}}$ is the glucose/biomass yield coefficient (g-substrate/g-biomass), and $m_{Ec,S_{G_1}}$ is the maintenance coefficient (g-substrate/g-biomass/h).

1.4.2 *E. coli* saccharide uptake

Substrate uptake is assumed to be stoichiometrically coupled to growth. Additionally, experimental data for *E. coli* demonstrates non-growth associated substrate uptake (i.e. during stationary phase) for maintenance / isobutanol production [8]. We then model uptake of glucose as follows:

$$r_{S_{G_1}}^{Ec} = Y_{S_{G_1}/C_{Ec}} K_{Ec,S_{G_1}}^{I} \frac{\mu_{max,Ec,S_{G_1}} S_{G_1}}{K_{Ec,S_{G_1}} + S_{G_1}} C_{Ec} + m_{Ec,S_{G_1}} \frac{S_{G_1}}{K_{Ec,S_{G_1}} + S_{G_1}} C_{Ec} \quad \text{(S50)}$$

where $r_{S_{G_1}}^{Ec}$ is the rate of total glucose uptake by *E. coli* (g/L/h), and the other terms are as described in previous sections.

1.4.3 *E. coli* isobutanol production

Unlike many metabolic products, isobutanol production is not stoichiometrically coupled to growth, since substantial isobutanol production is observed during stationary phase [8]. To account for this, all consumed substrates, both for growth and maintenance, will be assumed to be converted to isobutanol. For generality, we allow yield coefficients to vary between growth and non-growth associated substrate uptake:

$$\frac{dI}{dt} = Y_{I/S_{G_1}}^{growth} Y_{S_{G_1}/C_{Ec}} K_{Ec,S_{G_1}}^{I} \frac{\mu_{max,Ec,S_{G_1}} S_{G_1}}{K_{Ec,S_{G_1}} + S_{G_1}} C_{Ec} + Y_{I/S_{G_1}}^{maint} m_{Ec,S_{G_1}} \frac{S_{G_1}}{K_{Ec,S_{G_1}} + S_{G_1}} C_{Ec} \tag{S51}$$

where $Y_{I/S_{G_1}}^{growth}$ is the growth associated isobutanol/glucose yield coefficient (g-iButOH/g-substrate), $Y_{I/S_{G_1}}^{maint}$ is the non-growth (maintenance) isobutanol/glucose yield coefficient (g-iButOH/g-substrate), and other terms are as described previously. In the case of *E. coli* K12, both yield coefficients would be 0 (i.e. no isobutanol production).

1.5 Enzymatic cellulose hydrolysis: general framework

There are numerous models reported in literature for microbial growth on cellulose [7]. However, few of these models accounts for the hydrolysis of cellulose to soluble saccharides. Competition between *E. coli* and *T. reesei* for soluble saccharides is a crucial ecological interaction that needs to be accounted for to accurately predict population dynamics, behavior, and isobutanol production in the TrEc consortium. Enzymatic cellulose hydrolysis is a complex process that is poorly understood, and remains an active area of research [7]. There are two main classes of cellulase: endoglucanases and cellobiohydrolases (also known as exoglucanases) [7]. Most cellulolytic organisms produce multiple, even dozens of cellulases of each type [7]. As a starting point for developing mechanistic models of cellulose hydrolysis, we utilize the general framework for enzymatic cellulose hydrolysis proposed by [7] and [9], which we describe in the following sections. Additionally, we also include generalized soluble saccharide mole balances that describe rate of production/consumption due to enzymatic hydrolysis and microbial uptake.

1.5.1 Endoglucanase

Endoglucanases adsorb at random to cellulose molecules and cleave them to release two shorter chain polysaccharides [9]. This mechanism can be represented as [9]:

$$S_{G_i} + E_{EGm} \xleftarrow{K_{dis}^{EGm}} S_{G_i} \cdot E_{EGm} \xrightarrow{k_{EGm}} E_{EGm} + S_{G_{i-j}} + S_{G_j} \tag{S52}$$

where E_{EGm} is endoglucanase m, K_{dis}^{EGm} is the dissociation constant for endoglucanase m (mM bonds), k_{EGm} is the rate constant of adsorbed E_{EGm} (mmol-bonds/g-EGm·S_{G_i}/h), i and j are cellulose chain lengths, with $1 \leq j < i$, $S_{G_i} \cdot E_{EGm}$ is adsorbed E_{EGm}, and other terms are as previously described. The rate of hydrolysis of saccharide S_{G_i} by endoglucanase m is then [9]:

$$r_{S_{G_i}}^{EGm} = -k_{EGm} \left[S_{G_i} \cdot E_{EGm} \right] \tag{S53}$$

where $r_{S_{G_i}}^{EGm}$ is hydrolysis rate (mM-bonds/h) and $[S_{G_i} \cdot E_{EGm}]$ is the mass concentration of E_{EGm} adsorbed to S_{G_i} (g/L). Cellulose saccharides S_{G_i} can be formed from endoglucanase hydrolysis of longer cellulose molecules S_{G_k}, with $k > i$. The rate of hydrolysis of S_{G_k} to S_{G_i} is equal to the overall rate of hydrolysis of S_{G_k} times the fraction of hydrolysis events that lead to a chain length S_{G_i}, $f_{G_k \to G_i}$. If all glycosidic bonds are cleaved at an equal rate, then $f_{G_k \to G_i} = 2/\left(k-1\right)$, leading to the following [9]:

$$r_{S_{G_k} \to S_{G_i}}^{EGm} = f_{G_k \to G_i} r_{S_{G_k}}^{EGm} = -\frac{2}{k-1} k_{EGm} \left[S_{G_k} \cdot E_{EGm} \right] \tag{S54}$$

The overall rate of formation of S_{G_i} by endoglucanase is then the sum of the rate of hydrolysis of S_{G_i} and the rate of formation of S_{G_i} from S_{G_k} with $k > i$ [9]:

$$r_{S_{G_i}}^{EGm} = -k_{EGm}\left[S_{G_i} \cdot E_{EGm}\right] - \sum_{k>i} f_{G_k \to G_i} r_{S_{G_k}}^{EGm} \tag{S55}$$

$$= -k_{EGm}\left[S_{G_i} \cdot E_{EGm}\right] + \sum_{k>i} \frac{2}{k-1} k_{EGm}\left[S_{G_k} \cdot E_{EGm}\right] \tag{S56}$$

where the upper limit of the summation is implicitly understood as DP_{max} (maximum polysaccharide length i for given type of cellulose) and other terms are as described previously.

1.5.2 Exoglucanase

In contrast to endoglucanases, exoglucanases (often referred to as cellobiohydrolases) bind to the ends of cellulose chains and processively hydrolyze cellobiose units. Mechanistically, this can be represented as [9]:

$$S_{G_i} + E_{CBHm} \xleftrightarrow{K_{dis}^{CBHm}} S_{G_i} \cdot E_{CBHm} \xrightarrow{k_{CBHm}} E_{CBHm} + S_{G_{i-2}} + S_{G_2} \tag{S57}$$

where E_{CBHm} represents cellobiohydrolase m, K_{dis}^{CBHm} is the dissociation constant for cellobiohydrolase m (mM bonds), k_{CBHm} is the rate constant of adsorbed E_{CBHm} (mmol-bonds/g-CBHm·S_{G_i}/h), $S_{G_i} \cdot E_{CBHm}$ is adsorbed E_{EGm}, and the other terms are as described previously. The rate of hydrolysis of saccharide S_{G_i} by cellobiohydrolase is then [9]:

$$r_{S_{G_i} \to S_{G_2}}^{CBHm} = -k_{CBHm}\left[S_{G_i} \cdot E_{CBHm}\right] \tag{S58}$$

where terms are similar to those described for endoglucanase. S_{G_i} can also be formed from cellobiohydrolase hydrolysis of $i+2$ chain length cellulose molecules. The overall rate of formation of S_{G_i} by cellobiohydrolase is then the sum of the rate of hydrolysis of S_{G_i} and the rate of formation of S_{G_i} from $i+2$ saccharides [9]:

$$r_{S_{G_i}}^{CBHm} = -k_{CBHm}\left[S_{G_i} \cdot E_{CBHm}\right] + k_{CBHm}\left[S_{G_{i+2}} \cdot E_{CBHm}\right] \tag{S59}$$

where terms are as described in previous sections. The overall rate of formation of S_{G_2} is the sum of cellobiohydrolase hydrolysis rates for all saccharides S_{G_i} for $i \geq 3$:

$$r_{S_{G_2}}^{CBHm} = k_{CBHm} \sum_{i \geq 3} \left[S_{G_i} \cdot E_{CBHm}\right] \tag{S60}$$

where the upper limit of the summation is implicitly understood as DP_{max} and other terms are as described previously.

1.5.3 β-glucosidase

β-glucosidase hydrolyzes cellobiose and other soluble cellulose oligosaccharides to glucose [10]. For soluble saccharides of DP $i = 2..4$ this can be mechanistically represented as:

$$S_{G_i} + E_{BGLm} \xleftrightarrow{K_{G_i,dis}^{BGLm}} S_{G_i} \cdot E_{BGLm} \xrightarrow{k_{BGLm,G_i}} E_{BGLm} + S_{G_{i-1}} + S_{G_1} \tag{S61}$$

where E_{BGLm} represents β-glucosidase m, $K_{G_i,dis}^{BGLm}$ is the dissocation constant for β-glucosidase m (mM substrate), k_{BGLm,G_i} is the rate constant of adsorbed E_{BGLm} (mmol-bonds/g-BGLm·S_{G_i}/h), $S_{G_i} \cdot E_{BGLm}$ is the β-glucosidase / substrate complex, and the other terms are as described in previous sections. The rate of hydrolysis of S_{G_i} or formation of S_{G_1} is then:

$$r_{S_{G_i}}^{BGLm} = -r_{S_{G_1}}^{BGLm} = -k_{BGLm,G_i}\left[S_{G_i} \cdot E_{BGLm}\right] \tag{S62}$$

For cellobiose, $r_{S_{G_1}}^{BGLm} = 2k_{BGLm,G_2}\left[S_{G_2} \cdot E_{BGLm}\right]$ since two glucoses are produced per cellobiose.

1.5.4 Saccharide mass balances

In general, saccharide mass balances must account for both enzymatic cellulose hydrolysis and microbial saccharide uptake. However, insoluble cellulose molecules (chain length $i > 4$) are not utilized biologically. Thus for chain length $i > 4$ cellulose molecules, net rates of formation from endoglucanase and cellobiohydrolase need only be considered. Writing a mass balance for each cellulose molecule of chain length i with $i > 4$ yields [9]:

$$\frac{dS_{G_i}}{dt} = \sum_m r_{S_{G_i}}^{EGm} + \sum_n r_{S_{G_i}}^{CBHn} \text{ for } i > 4 \tag{S63}$$

where all terms are as described in previous sections. For the case of the *T. reesei* cellulase system, consisting of endoglucanase 1 ($EG1$), cellobiohydrolase 1 ($CBH1$), and cellobiohydrolase 2 ($CBH2$), the mass balances reduce to:

$$\frac{dS_{G_i}}{dt} = r_{S_{G_i}}^{EG1} + r_{S_{G_i}}^{CBH1} + r_{S_{G_i}}^{CBH2} \text{ for } i > 4 \tag{S64}$$

where all terms are as described in previous sections. For soluble saccharides, microbial saccharide uptake and β-glucosidase hydrolysis must also be considered. For a co-culture of *T. reesei* and *E. coli*, writing a mass balance on cellulose molecules of chain length $1 \leq i \leq 4$ yields:

$$\frac{dS_{G_i}}{dt} = r_{S_{G_i}}^{EG1} + r_{S_{G_i}}^{CBH1} + r_{S_{G_i}}^{CBH2} + r_{S_{G_i}}^{BGL} - \frac{1}{MW_{S_{G_i}}}\left(r_{S_{G_i}}^{Tr} + r_{S_{G_i}}^{Ec}\right) \text{ for } 1 \leq i \leq 4 \tag{S65}$$

where $MW_{S_{G_i}}$ is the molecular weight of S_{G_i} (g/mmol), and all other terms are as described in previous sections. Most *E. coli* strains cannot metabolize cellulose oligosaccharides and are thus only able to use S_{G_1}; additionally, while it seems biologically plausible, there is little evidence to support significant uptake and metabolism of $i > 2$ glucose saccharides by *T. reesei*. We thus reduce the $i \leq 4$ saccharide balances to:

$$\frac{dS_{G_i}}{dt} = r_{S_{G_i}}^{EG1} + r_{S_{G_i}}^{CBH1} + r_{S_{G_i}}^{CBH2} + r_{S_{G_i}}^{BGL} \text{ for } 3 \leq i \leq 4 \tag{S66}$$

$$\frac{dS_{G_2}}{dt} = r_{S_{G_2}}^{EG1} + r_{S_{G_2}}^{CBH1} + r_{S_{G_2}}^{CBH2} + r_{S_{G_2}}^{BGL} - \frac{1}{MW_{S_{G_2}}} r_{S_{G_2}}^{Tr} \tag{S67}$$

$$\frac{dS_{G_1}}{dt} = r_{S_{G_1}}^{EG1} + r_{S_{G_1}}^{CBH1} + r_{S_{G_1}}^{CBH2} + r_{S_{G_1}}^{BGL} - \frac{1}{MW_{S_{G_1}}}\left(r_{S_{G_1}}^{Tr} + r_{S_{G_1}}^{Ec}\right) \tag{S68}$$

where all terms are as described in previous sections.

1.6 Enzymatic cellulose hydrolysis: kinetics and rate laws

Deriving tractable kinetic expressions for enzymatic cellulose hydrolysis requires making simplifying assumptions, many of which are idealizations that do not apply to real systems. Zhang and Lynd [9] derived rate laws for endoglucanase and exoglucanase by incorporating enzyme mass balances with adsorption equilibria and making the following simplifying assumptions:

1. Random adsorption.
2. Continuous equilibrium between adsorbed and free components.
3. No interactions between adsorbing components / affinity does not vary with fractional coverage.
4. Substrate binding sites are in excess of enzyme.
5. Constant substrate reactivity.
6. Negligible inhibition from hydrolysis products (e.g. S_{G_1} and S_{G_2}).

Some of the assumptions made in [9] are clearly not applicable to enzymatic cellulose hydrolysis in the TrEc consortium. In particular, the assumption of excess substrate binding sites is valid only in the early stages of growth; during later stages, when enzyme concentrations are maximal and cellulose concentrations low, substrate binding sites are clearly not in excess of enzyme binding sites [7]. Additionally, in real systems, substrate reactivity (defined in terms of apparent rate constants k) is found to decrease by one to two orders of magnitude as cellulose conversion approaches 100% [7].

To better model enzymatic cellulose hydrolysis with the TrEc consortium, we advanced Zhang and Lynd's model [9] by deriving a new set of kinetics for endoglucanase and exoglucanase. Our derivation incorporates substrate site balances and empirical correlations for declining reactivity, described below. As a secondary consideration, we also include empirical non-competitive product (S_{G_1} and S_{G_2}) inhibition expressions in our kinetics, though these terms are likely to be unimportant since soluble saccharide concentrations are generally low during TrEc consortium growth on cellulosic substrates.

1.6.1 Endoglucanase

As described in section 1.5.1, the overall rate of formation of S_{G_i} by endoglucanase is the sum of the hydrolysis rate of S_{G_i} and the rate of formation of S_{G_i} from S_{G_k} hydrolysis with $k > i$ [9]:

$$r_{S_{G_i}}^{EGm} = -k_{EGm}\left[S_{G_i} \cdot E_{EGm}\right] + \sum_{k>i} \frac{2}{k-1} k_{EGm}\left[S_{G_k} \cdot E_{EGm}\right] \tag{S56}$$

where the upper limit of the summation is implicitly understood as DP_{max} (maximum polysaccharide length i for given type of cellulose) and terms are as described previously. Computing $r_{S_{G_i}}^{EGm}$ requires us to express $[S_{G_i} \cdot E_{EGm}]$ in terms of known or measurable variables. Zhang and Lynd [9] derive such expressions by incorporating E_{EGm} mass balances with the E_{EGm} adsorption equilibrium, given below:

Adsorption equilibrium [9]:

$$K_{dis}^{EGm} = \frac{E_{EGm,f} C_f}{\sum\limits_{i\geq 2}\left[S_{G_i} \cdot E_{EGm}\right]} \tag{S69}$$

where $E_{EGm,f}$ is concentration of free (i.e. unadsorbed) endoglucanase m (g-EGm/L), C_f is concentration of free substrate binding sites (mM bonds), the upper limit of the summation is implicitly understood as DP_{max}, and other terms are as described previously.

Enzyme balance [9]:

$$E_{EGm} = E_{EGm,f} + \sum_{i\geq 2}\left[S_{G_i} \cdot E_{EGm}\right] \tag{S70}$$

where the upper limit of the summation is implicitly understood as DP_{max} and other terms are as described previously.

We modify the derivation described in [9] by incorporating a balance on substrate binding sites [9]:

$$\sum_{i\geq 2} F_a\,(i-1)\,S_{G_i} = \sum_{i\geq 2} 2\alpha_{EGm} \frac{\left[S_{G_i} \cdot E_{EGm}\right]}{MW_{EGm}} + C_f \tag{S71}$$

where F_a is the fraction of enzyme accessible β-glycosidic bonds, α_{EGm} is the number of cellobiose lattice units occupied by a single molecule of endoglucanase m, MW_{EGm} is the molecular weight of endoglucanase m (g-EGm/mmol), C_f is the concentration of free β-glycosidic bonds accessible to cellulase (mM bonds), and the upper limit of the summation is implicitly understood as DP_{max}. We then derive expressions for $[S_{G_i} \cdot E_{EGm}]$:

$$[S_{G_i} \cdot E_{EGm}] = \frac{(i-1)\, S_{G_i}}{\sum_{i\geq 2} (i-1)\, S_{G_i}} Y \tag{S72}$$

$$Y = \frac{1}{2} b_Y \pm \frac{1}{2} \sqrt{b_Y^2 - \frac{4}{\beta_{EGm}} E_{EGm} \sum_{i\geq 2} F_a\, (i-1)\, S_{G_i}} \tag{S73}$$

$$b_Y = E_{EGm} + \frac{K_{dis}^{EGm}}{\beta_{EGm}} + \frac{1}{\beta_{EGm}} \sum_{i\geq 2} F_a\, (i-1)\, S_{G_i} \tag{S74}$$

$$\beta_{EGm} = \frac{2\alpha_{EGm}}{MW_{EGm}} \tag{S75}$$

where all terms are as described previously. Incorporating balances on both enzyme binding sites and substrate binding sites into the adsorption equilibrium expression results in a quadratic equation in $[S_{G_i} \cdot E_{EGm}]$; the physically meaningful root of Y is the one for which binding site balances are satisfied: $0 < [S_{G_i} \cdot E_{EGm}] < E_{EGm}$ and $0 < [S_{G_i} \cdot E_{EGm}] < (1/\beta_{EGm}) \sum_{i\geq 2} F_a\, (i-1)\, S_{G_i}$ [7].

The overall rate of formation of S_{G_i} due to endoglucanase is then:

$$r_{S_{G_i}}^{EGm} = \frac{k_{EGm} Y}{\sum_{i\geq 2} (i-1)\, S_{G_i}} \left(2 \sum_{k>i} S_{G_k} - (i-1)\, S_{G_i} \right) \tag{S76}$$

where all terms are as described previously.

1.6.2 Exoglucanase

As described in section 1.5.2, the overall rate of formation of S_{G_i} by cellobiohydrolase is the sum of the hydrolysis rate of S_{G_i} and the rate of formation of S_{G_i} from hydrolysis of $i+2$ saccharides [9]:

$$r_{S_{G_i}}^{CBHm} = -k_{CBHm} [S_{G_i} \cdot E_{CBHm}] + k_{CBHm} \left[S_{G_{i+2}} \cdot E_{CBHm} \right] \tag{S59}$$

Computing $r_{S_{G_i}}^{CBHm}$ requires us to express $[S_{G_i} \cdot E_{CBHm}]$ in terms of known or measurable variables. Zhang and Lynd [9] derive expressions for $[S_{G_i} \cdot E_{CBHm}]$ analogous to the above described procedure for endoglucanase, that is by incorporating E_{CBHm} mass balances with E_{CBHm} adsorption equilibrium, shown below:

Adsorption equilibrium [9]:

$$K_{dis}^{CBHm} = \frac{E_{CBHm,f} C_f}{\sum_{i\geq 3} [S_{G_i} \cdot E_{CBHm}]} \tag{S77}$$

where $E_{CBHm,f}$ is concentration of free (i.e. unbound) cellobiohydrolase m (g-CBHm/L), C_f is concentration of free substrate sites (mM bonds), the upper limit of the summation is implicitly understood as DP_{max}, and other terms are as described previously.

Enzyme balance [9]:

$$E_{CBHm} = E_{CBHm,f} + \sum_{i\geq 3} [S_{G_i} \cdot E_{CBHm}] \tag{S78}$$

where terms are as described previously.

We modify the approach described in [9] by including a balance on substrate binding sites [9]:

$$\sum_{i\geq 3} 2 F_a S_{G_i} = \sum_{i\geq 3} \frac{[S_{G_i} \cdot E_{CBHm}]}{MW_{CBHm}} + C_f \tag{S79}$$

where MW_{CBHm} is the molecular weight of cellobiohydrolase m (g-CBHm/mmol), the upper limit of the summation is implicitly understood as DP_{max}, and other terms are as described previously. Note that we assume cellobiohydrolases adsorb only at cellulose chain ends. We then derive expressions for $[S_{G_i} \cdot E_{CBHm}]$:

$$[S_{G_i} \cdot E_{CBHm}] = \frac{S_{G_i}}{\sum\limits_{i\geq 3} S_{G_i}} Z \tag{S80}$$

$$Z = \frac{1}{2} b_Z \pm \frac{1}{2} \sqrt{b_Z^2 - \frac{8 F_a E_{CBHm}}{\beta_{CBHm}} \sum_{i\geq 3} S_{G_i}} \tag{S81}$$

$$b_Z = E_{CBHm} + \frac{K_{dis}^{CBHm}}{\beta_{CBHm}} + \frac{2F_a}{\beta_{CBHm}} \sum_{i\geq 3} S_{G_i} \tag{S82}$$

where $\beta_{CBHm} = 1/MW_{CBHm}$ and all other all terms are as described in previous sections. Incorporating balances on both enzyme binding sites and substrate binding sites into the adsorption equilibrium expression results in a quadratic equation in $[S_{G_i} \cdot E_{CBHm}]$; the physically meaningful root of Z is the one for which binding site balances are satisfied: $0 < [S_{G_i} \cdot E_{CBHm}] < E_{CBHm}$ and $0 < [S_{G_i} \cdot E_{CBHm}] < MW_{CBHm} \sum\limits_{i=n} 2F_a S_{G_i}$ [7]. The overall rate of formation of S_{G_i} by cellobiohydrolase is the sum of the hydrolysis rate of S_{G_i} and the rate of formation of S_{G_i} from hydrolysis of $i+2$ saccharides:

$$r_{S_{G_i}}^{CBHm} = \frac{k_{CBHm} Z}{\sum\limits_{i\geq 3} S_{G_i}} \left(S_{G_{i+2}} - S_{G_i} \right) \tag{S83}$$

where all terms are as described previously. The overall rate of formation of S_{G_2} is the sum of cellobiohydrolase hydrolysis rates for all saccharides S_{G_i} for $i \geq 3$:

$$r_{S_{G_2}}^{CBHm} = k_{CBHm} Z \tag{S84}$$

where all terms are as described previously.

1.6.3 β-glucosidase

We adopt multisubstrate Michaelis-Menten kinetics for β-glucosidase [10]:

$$r_{S_{G_i}}^{BGLm} = -\frac{k_{BGLm,G_i} E_{BGLm} S_{G_i}}{K_{M,G_i}^{BGLm} \left(1 + \frac{S_{G_1}}{K_{G_1}^{BGLm}} \sum\limits_{i=2}^{4} \frac{S_{G_i}}{K_{M,G_i}^{BGLm}} \right)} \tag{S85}$$

where K_{M,G_i}^{BGLm} is the Michaelis constant for S_{G_i} (mM), $K_{G_1}^{BGLm}$ is the glucose inhibition term (mM), and other terms are as described in previous sections. The total rate of glucose production via β-glucosidase is then:

$$r_{S_{G_1}}^{BGLm} = -2 r_{S_{G_2}}^{BGLm} - \sum_{i=2}^{4} r_{S_{G_i}}^{BGLm} \tag{S86}$$

1.6.4 Empirical relations for substrate reactivity and product inhibition

Declining substrate reactivity It has long been observed that specific rates of cellulose hydrolysis (i.e. rate per adsorbed cellulase) decline by one to two orders of magnitude as the reaction proceeds to completion [7]. Numerous explanations for this phenomenon have been proposed, but presently the most widely accepted theory is declining substrate reactivity [7]. Whatever the cause, the phenomenon can be empirically modeled. We adopt the following model which describes rate constants for cellulose hydrolysis as a function of substrate conversion [11]:

$$k_m = k_{m,max} \left[f_{deact} \left(1 - X \right)^{n_{deact,m}} + \left(1 - f_{deact} \right) \right] \tag{S87}$$

$$X = \frac{\sum\limits_{i>4} MW_{G_i} \left(S_{G_i}|_{t_0} - S_{G_i}|_t\right)}{\sum\limits_{i>4} MW_{G_i} S_{G_i}|_{t_0}} \tag{S88}$$

where k_m is the apparent rate constant for enzyme m ($m = EG1$, $CBH1$, or $CBH2$ in the case of the *T. reesei* cellulase system; mmol-bonds/g-m/h), $k_{m,max}$ the maximum rate constant for enzyme m (i.e. at 0% conversion; mmol-bonds/g-m/h), $1 - f_{deact}$ is fractional residual activity, $n_{deact,m}$ is an empirically determined exponent for cellulase m, X is substrate conversion (g-consumed/g-initial), MW_{G_i} is the molecular weight of saccharide G_i (g/mmol), $S_{G_i}|_{t_0}$ is the initial concentration of saccharide G_i (mM), $S_{G_i}|_t$ is the concentration of saccharide G_i at time t (mM), and the upper limit of the summation is implicitly understood as DP_{max}.

Product inhibition Glucose and cellobiose have been observed to non-competitively inhibit most cellulase enzymes [7]. Expressions for inhibition can be formally derived from reaction mechanisms; rather than performing a formal derivation for each enzyme, we empirically describe non-competitive inhibition in terms of an apparent reaction rate constant [12]:

$$k_m = \frac{k_{m,max}}{1 + \frac{S_{G_1}}{K^m_{G_1}} + \frac{S_{G_2}}{K^m_{G_2}}} \tag{S89}$$

where $K^m_{G_1}$ and $K^m_{G_2}$ are dissociation constants between enzyme m ($m = EG1$, $CBH1$, or $CBH2$ in the case of the *T. reesei* cellulase system; g/L or mM) and S_{G_1} and S_{G_2} respectively, and all other terms are as described previously. During microbial growth on cellulose, soluble saccharide concentrations are likely to be very low, so accounting for product inhibition is probably unimportant. However, for completeness we include inhibition in our model.

Combined expression for declining reactivity and substrate inhibition The above empirical expressions can be combined to describe effects of declining substrate reactivity and product inhibition on reaction rate constants:

$$k_m = k_{m,max} \left[\frac{f_{deact} \left(1 - X\right)^{n_{deact,m}} + \left(1 - f_{deact}\right)}{1 + \frac{S_{G_1}}{K^m_{G_1}} + \frac{S_{G_2}}{K^m_{G_2}}} \right] \tag{S90}$$

where all terms are as described previously.

1.7 Model summary

We provide a brief synopsis of our modeling framework in this section. **See preceding sections for a full description of our model, including mass transfer analysis of the *T. reesei* cell surface, rate law expressions and derivations, and discussion of semi-mechanistic enzymatic cellulose hydrolysis models.** For details regarding implementation of the model in MATLAB, see section 2.1. To summarize, we developed a comprehensive ordinary differential equation (ODE) modeling framework that captures salient features of the TrEc consortium. We derived rate expressions for microbial growth, microbial uptake of soluble saccharides, production of cellulase enzymes (endoglucanase, exoglucanase, and β-glucosidase) by *T. reesei*, enzymatic cellulose hydrolysis (based on novel semi-mechanistic models for each type of enzyme), isobutanol production by *E. coli*, and isobutanol toxicity. The model was developed by writing differential mole/mass balances (for a batch reactor) for each species of interest, including microbial biomass (*T. reesei* and *E. coli*), cellulase enzymes, insoluble cellulose polysaccharides, soluble oligo and monosaccharides, and isobutanol. Our model explicitly accounts for each possible cellulose saccharide S_{G_i}, where i is the number of glucose monomers. Thus the total number of ODEs will depend on the degree of polymerization (DP) distribution of S_{G_i}, which varies between different cellulosic substrates. For a given S_{G_i} distribution, a total of $5 + DP_{max}$ ODEs are required, where DP_{max} is the maximum DP of the cellulosic substrate. We give a brief overview of our modeling framework in the following sections, including key mole/mass balances.

Note: equation numbers in this summary correspond to those in the preceding sections.

1.7.1 *T. reesei* biomass balances

T. reesei is a multicellular filamentous fungus that has different mycelial growth states. Vegetative growth and enzyme secretion are highly active at hyphal tips, while senescent mycelium is relatively dormant [5]. Assuming that growth at hyphal tips follows Monod kinetics and that *T. reesei* is capable of simultaneous utilization of multiple soluble sugars (i.e. glucose and soluble glucose oligosaccharides), *T. reesei* growth in the presence of isobutanol can be described with a segregated kinetic model:

$$\frac{dC_{Tr,v}}{dt} = \mu_{Tr} C_{Tr,v} - k_{v\to s} C_{Tr,v} \tag{S40}$$

$$\frac{dC_{Tr,s}}{dt} = k_{v\to s} C_{Tr,v} - k_{Tr,d} C_{Tr,s} \tag{S41}$$

where $C_{Tr,v}$ is vegetative mycelium concentration (g/L), μ_{Tr} is a generalized Monod function (1/h) depending on isobutanol concentration I (g/L) and concentration of soluble glucose saccharides S_{G_i} (g/L; i is the number of sugar monomers), $k_{v\to s}$ is the specific rate of conversion of vegetative mycelium to senescent mycelium (1/h), $C_{Tr,s}$ is the concentration of senescent mycelium (g/L), and $k_{Tr,d}$ is the specific death rate of senescent mycelium (1/h). See section 1.3.1 for further details.

1.7.2 Enzyme balances

Assuming that enzyme secretion is stoichiometrically coupled to growth and that composition of secreted enzymes is constant, the following expression can be derived for cellulase production:

$$\frac{dE_T}{dt} = Y_{E_T/C_{Tr}} \mu_{Tr} C_{Tr,v} + k_{E_T} C_{Tr,s} \tag{S44}$$

$$\frac{dE_i}{dt} = x_{E_i} \frac{dE_T}{dt} = x_{E_i} \left[Y_{E_T/C_{Tr}} \mu_{Tr} C_{Tr,v} + k_{E_T} C_{Tr,s} \right] \tag{S45}$$

where E_T is the total concentration of secreted enzymes (g/L), $Y_{E_T/C_{Tr}}$ is the enzyme/biomass yield coefficient (g-enzyme/g-biomass), k_{E_T} is the specific enzyme production rate of senescent mycelium (g-enzyme/g-biomass/h), E_i is concentration of enzyme i (g/L), and x_{E_i} is the fraction of enzyme i in the total enzyme secretome (E_i/E_T). Our model accounts for the major *T. reesei* cellulases: cellobiohydrolase I ($i = CBH1$), cellobiohydrolase II ($i = CBH2$), endoglucanase I ($i = EG1$), and β-glucosidase 1 ($i = BGL$). See section 1.3.2 for further details.

1.7.3 Enzymatic cellulose hydrolysis

We utilize the general framework for enzymatic cellulose hydrolysis proposed by [7] and [9] to derive semi-mechanistic rate laws for each type of cellulase (endoglucanase, exoglucanase, and β-glucosidase), as summarized below:

Endoglucanase Endoglucanases adsorb at random to cellulose molecules and cleave them to release two shorter chain polysaccharides [9]:

$$S_{G_i} + E_{EGm} \xleftrightarrow{K_{dis}^{EGm}} S_{G_i} \cdot E_{EGm} \xrightarrow{k_{EGm}} E_{EGm} + S_{G_{i-j}} + S_{G_j} \tag{S52}$$

where E_{EGm} is endoglucanase m, S_{G_n} are cellulose polysaccharides, K_{dis}^{EGm} is the dissociation constant for endoglucanase m (mM bonds), k_{EGm} is the rate constant of adsorbed E_{EGm} (mmol-bonds/g-EGm·S_{G_i}/h), i and j are cellulose chain lengths (with $1 \leq j < i$), $S_{G_i} \cdot E_{EGm}$ is adsorbed E_{EGm}, and other terms are as previously described. The overall rate of formation of S_{G_i} by endoglucanase is then the sum of the rate of hydrolysis of S_{G_i} and the rate of formation of S_{G_i} from S_{G_k} with $k > i$. The hydrolysis rate of S_{G_k} to S_{G_i} is equal to the overall hydrolysis rate of S_{G_k} times the fraction of hydrolysis events that lead to a chain length S_{G_i}, $f_{G_k\to G_i}$. If all glycosidic bonds are cleaved at an equal rate, then $f_{G_k\to G_i} = 2/(k-1)$, leading to the following [9]:

$$r_{S_{G_i}}^{EGm} = -k_{EGm}\left[S_{G_i} \cdot E_{EGm}\right] - \sum_{k>i} f_{G_k \to G_i} r_{S_{G_k}}^{EGm} \tag{S55}$$

$$= -k_{EGm}\left[S_{G_i} \cdot E_{EGm}\right] + \sum_{k>i} \frac{2}{k-1} k_{EGm}\left[S_{G_k} \cdot E_{EGm}\right] \tag{S56}$$

where $r_{S_{G_i}}^{EGm}$ is hydrolysis rate (mM-bonds/h), $[S_{G_i} \cdot E_{EGm}]$ is the mass concentration of E_{EGm} adsorbed to S_{G_i} (g/L), the upper limit of the summation is implicitly understood as DP_{max}, and other terms are as described previously. We developed expressions for $[S_{G_i} \cdot E_{EGm}]$ in terms of measurable variables by incorporating enzyme mass balances and substrate binding site balances with the endoglucanase adsorption equilibria. **See section 1.6.1 for derivation and final rate law expression.**

Exoglucanase In contrast to endoglucanases, exoglucanases (often referred to as cellobiohydrolases) bind to the ends of cellulose chains and processively hydrolyze cellobiose units. Mechanistically, this can be represented as [9]:

$$S_{G_i} + E_{CBHm} \xleftrightarrow{K_{dis}^{CBHm}} S_{G_i} \cdot E_{CBHm} \xrightarrow{k_{CBHm}} E_{CBHm} + S_{G_{i-2}} + S_{G_2} \tag{S57}$$

where terms are analogous to those described for endoglucanase. The overall rate of formation of S_{G_i} by cellobiohydrolase is then the sum of the rate of hydrolysis of S_{G_i} and the rate of formation of S_{G_i} from $i+2$ saccharides [9]:

$$r_{S_{G_i}}^{CBHm} = -k_{CBHm}\left[S_{G_i} \cdot E_{CBHm}\right] + k_{CBHm}\left[S_{G_{i+2}} \cdot E_{CBHm}\right] \tag{S59}$$

where terms are analogous to those described for endoglucanase. The overall rate of formation of S_{G_2} is the sum of cellobiohydrolase hydrolysis rates for all saccharides S_{G_i} for $i \geq 3$:

$$r_{S_{G_2}}^{CBHm} = k_{CBHm} \sum_{i \geq 3} \left[S_{G_i} \cdot E_{CBHm}\right] \tag{S60}$$

where the upper limit of the summation is implicitly understood as DP_{max} and other terms are as described previously. Similar to our endoglucanase deriviation, we developed expressions for $[S_{G_i} \cdot E_{CBHm}]$ in terms of measurable variables by incorporating enzyme mass balances and substrate binding site balances with exoglucanase adsorption equilibria. **See section 1.6.2 for derivation and final rate law expression.**

β-glucosidase β-glucosidase hydrolyzes cellobiose and other soluble cellulose oligosaccharides to glucose [10]. For soluble saccharides of DP $i = 2..4$ this can be mechanistically represented as:

$$S_{G_i} + E_{BGLm} \xleftrightarrow{K_{G_i,dis}^{BGLm}} S_{G_i} \cdot E_{BGLm} \xrightarrow{k_{BGLm,G_i}} E_{BGLm} + S_{G_{i-1}} + S_{G_1} \tag{S61}$$

where terms are analogous to those described above. The rate of hydrolysis of S_{G_i} or formation of S_{G_1} is then:

$$r_{S_{G_i}}^{BGLm} = -r_{S_{G_1}}^{BGLm} = -k_{BGLm,G_i}\left[S_{G_i} \cdot E_{BGLm}\right] \tag{S62}$$

where terms are analogous to those described above. For cellobiose, $r_{S_{G_1}}^{BGLm} = 2k_{BGLm,G_2}\left[S_{G_2} \cdot E_{BGLm}\right]$ since two glucoses are produced per cellobiose. See section 1.6.3 for further description of β-glucosidase rate laws.

1.7.4 *E. coli* biomass balance

We assume that *E. coli* utilizes only glucose for growth (i.e. cannot metabolize glucose oligocaccharides). Growth can be then be reasonably modeled with Monod kinetics [1]:

$$\frac{dC_{Ec}}{dt} = \left(\mu_{Ec} - k_{Ec,d}\right) C_{Ec} \tag{S47}$$

where C_{Ec} is the concentration of *E. coli* (g/L), μ_{Ec} is specific growth rate (1/h), and $k_{Ec,d}$ is the specific cell death rate (1/h). μ_{Ec} is assumed to be a function of glucose concentration S_{G1} (g/L), with concentration-dependent inhibition from isobutanol; see section 1.4.1 for further details.

1.7.5 Isobutanol mass balance

Unlike many metabolic products, isobutanol production is not stoichiometrically coupled to growth, since substantial isobutanol production is observed during stationary phase [8]. To account for this, all consumed substrates, for both growth and maintenance, will be assumed to be converted to isobutanol; for generality, we allow yield coefficients to vary between growth and non-growth associated substrate uptake. Accounting for both growth and maintenance associated isobutanol production yields the following mass balance:

$$\frac{dI}{dt} = Y_{I/S_{G_1}}^{growth} Y_{S_{G_1}/C_{Ec}} \mu_{Ec} C_{Ec} + Y_{I/S_{G_1}}^{maint} m_{Ec,S_{G_1}} \frac{S_{G_1}}{K_{Ec,S_{G_1}} + S_{G_1}} C_{Ec} \tag{S51}$$

where $Y_{I/S_{G_1}}^{growth}$ is the growth associated isobutanol/glucose yield coefficient (g-iButOH/g-substrate), $K_{Ec,S_{G_1}}$ is glucose affinity (g/L), $m_{Ec,S_{G_1}}$ is the maintenance coefficient (g-substrate/g-biomass/h), and $Y_{I/S_{G_1}}^{maint}$ is the non-growth (maintenance) isobutanol/glucose yield coefficient (g-iButOH/g-substrate), and other terms are as described previously. In the case of *E. coli* K12, yield coefficients are 0 (i.e. no isobutanol production). See section 1.4.3 for further details.

1.7.6 Cellulose polysaccharide (DP>4) mole balances

In general, saccharide mass balances must account for both enzymatic cellulose hydrolysis and microbial saccharide uptake. However, insoluble cellulose molecules (chain length $i > 4$) are not utilized biologically. Thus for chain length $i > 4$ cellulose molecules, net rates of formation from endoglucanase and cellobiohydrolase need only be considered. Writing a mole balance for each cellulose molecule of chain length i with $i > 4$ yields:

$$\frac{dS_{G_i}}{dt} = r_{S_{G_i}}^{EG1} + r_{S_{G_i}}^{CBH1} + r_{S_{G_i}}^{CBH2} \text{ for } i > 4 \tag{S64}$$

where S_{G_i} is the concentration of saccharide i (mM), $r_{S_{G_i}}^{EG1}$ is hydrolysis rate of saccharide i by endoglucanase I (mM/h; section 1.6.1), $r_{S_{G_i}}^{CBH1}$ is hydrolysis rate of saccharide i by cellobiohydrolase I (mM/h; section 1.6.2), and $r_{S_{G_i}}^{CBH2}$ is hydrolysis rate of saccharide i by cellobiohydrolase II (mM/h; section 1.6.2). See section 1.5.4 for further details.

1.7.7 Soluble mono and oligosaccharide (DP≤ 4) mole balances

For soluble saccharides, microbial saccharide uptake and β-glucosidase hydrolysis must also be considered. Most *E. coli* strains cannot metabolize cellulose oligosaccharides and are thus only able to use S_{G_1}; additionally, while it seems biologically plausible, there is little evidence to support significant uptake and metabolism of $i > 2$ glucose saccharides by *T. reesei*. Writing mole balances for saccharides $i \leq 4$ based on the preceding assumptions yields:

$$\frac{dS_{G_i}}{dt} = r_{S_{G_i}}^{EG1} + r_{S_{G_i}}^{CBH1} + r_{S_{G_i}}^{CBH2} + r_{S_{G_i}}^{BGL} \text{ for } 3 \leq i \leq 4 \tag{S66}$$

$$\frac{dS_{G_2}}{dt} = r_{S_{G_2}}^{EG1} + r_{S_{G_2}}^{CBH1} + r_{S_{G_2}}^{CBH2} + r_{S_{G_2}}^{BGL} - \frac{1}{MW_{S_{G_2}}} r_{S_{G_2}}^{Tr} \tag{S67}$$

$$\frac{dS_{G_1}}{dt} = r_{S_{G_1}}^{EG1} + r_{S_{G_1}}^{CBH1} + r_{S_{G_1}}^{CBH2} + r_{S_{G_1}}^{BGL} - \frac{1}{MW_{S_{G_1}}} \left(r_{S_{G_1}}^{Tr} + r_{S_{G_1}}^{Ec} \right) \tag{S68}$$

where S_{G_i} is the concentration of saccharide i, $r_{S_{G_i}}^{EG1}$ is hydrolysis rate of saccharide i by endoglucanase I (mM/h; section 1.6.1), $r_{S_{G_i}}^{CBH1}$ is hydrolysis rate of saccharide i by cellobiohydrolase I (mM/h; section 1.6.2), $r_{S_{G_i}}^{CBH2}$ is hydrolysis rate of saccharide i by cellobiohydrolase II (mM/h; section 1.6.2), $r_{S_{G_i}}^{BGL}$ is hydrolysis rate of saccharide i by β-glucosidase I (mM/h; section 1.6.3), $MW_{S_{G_i}}$ is molecular weight of saccharide i (g/mmol), $r_{S_{G_i}}^{Tr}$ is uptake rate

of saccharide i by *T. reesei* (g/L/h; section 1.3.3), and $r_{S_{G_1}}^{Ec}$ is uptake rate of glucose by *E. coli* (g/L/h; section 1.4.2). See section 1.5.4 for further details.

1.8 Simplified TrEc consortium model for stability analysis

We developed an abridged model of the TrEc consortium to facilitate stability analysis and investigation of cooperator-cheater dynamics. We utilized versions of this model with and without isobutanol production and toxicity effects. We model organism growth and substrate uptake with Monod kinetics; for simplicity we neglect maintenance substrate uptake. To reduce model complexity, we simplified cellulase kinetics to a single Michaelis-Menten rate law in terms of total cellulose concentration and total cellulase concentration; we assume cellulose is hydrolyzed to cellobiose, which is then hydrolyzed to glucose via β-glucosidase; all other polysaccharide intermediates are lumped into the cellulose term. A description of the model is given in the following sections.

1.8.1 *T. reesei* growth and substrate uptake

We model *T. reesei* growth and substrate uptake using Monod kinetics. For simplicity we neglect different mycelium types and assume that glucose is the sole growth substrate. An important subtlety is that cellobiose is hydrolyzed to glucose via cell-wall localized β-glucosidase of *T. reesei* [3], as depicted in Fig S1. This leads to locally increased concentration of glucose at the cell surface relative to the bulk media, thus affording privileged access to *T. reesei*. **We used the mass-transfer analysis described in section 1.2.2 to estimate glucose concentration at the cell surface.** *T. reesei* growth and substrate uptake rates are then:

$$\frac{dC_{Tr}}{dt} = \frac{\mu_{max,Tr}\left(S_{G_1} + \theta_{G_2 \to G_1} S_{G_2}\right)}{K_{S,Tr} + S_{G_1} + \theta_{G_2 \to G_1} S_{G_2}} C_{Tr} \tag{S91}$$

and

$$\begin{aligned} r_{S_{G_1}}^{Tr} &= Y_{S_{G_1}/C_{Tr}} \mu_{Tr} C_{Tr} \\ &= Y_{S_{G_1}/C_{Tr}} \frac{\mu_{max,Tr}\left(S_{G_1} + \theta_{G_2 \to G_1} S_{G_2}\right)}{K_{S,Tr} + S_{G_1} + \theta_{G_2 \to G_1} S_{G_2}} C_{Tr} \end{aligned} \tag{S92}$$

where all terms are analogous to those defined previously.

1.8.2 *E. coli* growth and substrate uptake

We use Monod kinetics to model *E. coli* growth and substrate uptake as:

$$\frac{dC_{Ec}}{dt} = \frac{\mu_{max,Ec} S_{G_1}}{K_{S,Ec} + S_{G_1}} C_{Ec} \tag{S93}$$

and

$$\begin{aligned} r_{S_{G_1}}^{Ec} &= Y_{S_{G_1}/C_{Ec}} \mu_{Ec} C_{Ec} \\ &= Y_{S_{G_1}/C_{Ec}} \frac{\mu_{max,Ec} S_{G_1}}{K_{S,Ec} + S_{G_1}} C_{Ec} \end{aligned} \tag{S94}$$

where all terms are analogous to those defined previously.

1.8.3 Enzyme production by *T. reesei*

We assume that enzyme secretion by *T. reesei* is directly coupled to growth:

$$\begin{aligned} \frac{dE_{cel}}{dt} &= Y_{E_{cel}/C_{Tr}} \mu_{Tr} C_{Tr} \\ &= Y_{E_{cel}/C_{Tr}} \frac{\mu_{max,Tr}\left(S_{G_1} + \theta_{G_2 \to G_1} S_{G_2}\right)}{K_{S,Tr} + S_{G_1} + \theta_{G_2 \to G_1} S_{G_2}} C_{Tr} \end{aligned} \tag{S95}$$

and

$$\begin{aligned}\frac{dE_{BGL}}{dt} &= Y_{E_{BGL}/C_{Tr}}\mu_{Tr}C_{Tr} \\ &= Y_{E_{BGL}/C_{Tr}}\frac{\mu_{max,Tr}\left(S_{G_1}+\theta_{G_2\to G_1}S_{G_2}\right)}{K_{S,Tr}+S_{G_1}+\theta_{G_2\to G_1}S_{G_2}}C_{Tr}\end{aligned} \tag{S96}$$

where E_{cel} is total cellulase (i.e. endoglucanase and exoglucanase) concentration (g/L), E_{BGL} is total β-glucosidase concentration (g/L), $Y_{E_{cel}/C_{Tr}}$ is the cellulase / biomass yield coefficient (g-cellulase/g-biomass), $Y_{E_{BGL}/C_{Tr}}$ is the β-glucosidase / biomass yield coefficient (g-β-glucosidase/g-biomass) and other terms are as defined previously. Due to the direct coupling between *T. reesei* growth and enzyme production, we can write enzyme concentration as:

$$E_{cel} = Y_{E_{cel}/C_{Tr}}C_{Tr} \tag{S97}$$

$$E_{BGL} = Y_{E_{BGL}/C_{Tr}}C_{Tr} \tag{S98}$$

1.8.4 Cellulose hydrolysis

We describe cellulase kinetics using a Michaelis-Menten rate law. For simplicity we neglect different types of cellulases, declining reactivity with conversion, and product inhibition, and lump all polysaccharides into a single cellulose concentration variable:

$$r^{cel}_{S_{G_2}} = -r^{cel}_{C} = \frac{k_{cel}E_{cel}S_C}{K_{M,cel}+S_C} \tag{S99}$$

where $r^{cel}_{S_{G_2}}$ is cellobiose production rate (g/L/h), r^{cel}_{C} is cellulose hydrolysis rate (g/L/h), k_{cel} is the rate constant (g/g-cellulase/h), S_C is total cellulose concentration (all polysaccharides with $DP > 2$; g/L), and $K_{M,cel}$ is cellulase affinity (g/L).

1.8.5 Cellobiose hydrolysis

We describe β-glucosidase kinetics using a Michaelis-Menten rate law:

$$r^{BGL}_{S_{G_1}} = -r^{BGL}_{S_{G_2}} = \frac{k_{BGL}E_{BGL}S_{G_2}}{K_{M,BGL}+S_{G_2}} \tag{S100}$$

where $r^{BGL}_{S_{G_1}}$ is glucose production rate (g/L/h), k_{BGL} is the rate constant (g/g-β-glucosidase/h), $K_{M,BGL}$ is β-glucosidase affinity (g/L), and other terms are as described previously.

1.8.6 Cellobiose mass balance

We write a mass balance on cellobiose accounting for production via cellulose hydrolysis and consumption via β-glucosidase hydrolysis:

$$\begin{aligned}\frac{dS_{G_2}}{dt} &= r^{cel}_{S_{G_2}} - r^{BGL}_{S_{G_2}} \\ &= \frac{k_{cel}E_{cel}S_C}{K_{M,cel}+S_C} - \frac{k_{BGL}E_{BGL}S_{G_2}}{K_{M,BGL}+S_{G_2}}\end{aligned} \tag{S101}$$

where all terms are as described previously

1.8.7 Glucose mass balance

We write a mass balance on glucose accounting for production via cellobiose hydrolysis and microbial consumption:

$$\begin{aligned}\frac{dS_{G_1}}{dt} &= r^{BGL}_{S_{G_1}} - r^{Ec}_{S_{G_1}} - r^{Tr}_{S_{G_1}} \\ &= \frac{k_{BGL}E_{BGL}S_{G_2}}{K_{M,BGL}+S_{G_2}} - Y_{S_{G_1}/C_{Ec}}\frac{\mu_{max,Ec}S_{G_1}}{K_{S,Ec}+S_{G_1}}C_{Ec} \\ &\quad - Y_{S_{G_1}/C_{Tr}}\frac{\mu_{max,Tr}\left(S_{G_1}+\theta_{G_2\rightarrow G_1}S_{G_2}\right)}{K_{S,Tr}+S_{G_1}+\theta_{G_2\rightarrow G_1}S_{G_2}}C_{Tr}\end{aligned} \tag{S102}$$

where all terms are as described previously.

1.8.8 Isobutanol production/toxicity effects

We utilize versions of this model with and without isobutanol production and toxicity effects (i.e. RUTC30/NV3 vs. RUTC30/K12 bicultures). We assume growth-coupled production of isobutanol by *E. coli*. For sake of simplicity, our abridged model does not include maintenance substrate uptake or isobutanol production. Isobutanol production rate is then given by:

$$\frac{dI}{dt} = Y_{I/S_{G_1}}r^{Ec}_{S_{G_1}} \tag{S103}$$

where I is isobutanol concentration (g/L), $Y_{I/S_{G_1}}$ is the isobutanol yield coefficient (g-iButOH/g-glucose), and $r^{Ec}_{S_{G_1}}$ is the *E. coli* glucose uptake rate (g/L/h). For *E. coli* NV3 pSA55/69, $Y_{I/S_{G_1}} = 0.25$ g-iButOH/g-glucose. We model isobutanol toxicity with empirical growth inhibition functions similar to Equations S42 & S48:

$$K^I_{Sp} = \begin{cases}\left(1-\frac{I}{I^*_{Sp}}\right)^{n_{Sp}} & \text{if } I \le I^*_{Sp} \\ 0 & \text{if } I > I^*_{Sp}\end{cases} \tag{S104}$$

where Sp is species (*E. coli* or *T. reesei*), I is isobutanol concentration (g/L), I^*_{Sp} is the growth inhibiting isobutanol concentration (g/L) for species Sp, and n_{Sp} is an empirical exponent for species Sp. Overall growth rates are given by:

$$\frac{dC_{Sp}}{dt} = K^I_{Sp}\mu_{Sp}C_{Sp} \tag{S105}$$

where C_{Sp} is concentration of species Sp and μ_{Sp} is the growth rate (i.e. Monod function, see Equations S91 & S93 in section 1.8). I^*_{Sp} and n_{Sp} values for *E. coli* NV3 pSA55/69 and *T. reesei* RUTC30 are given in Table S5.

2 Model analysis

2.1 Implementation and numerical solutions of TrEc consortium model

The ODE modeling framework described in section 1.7 was implemented in MATLAB (MathWorks Inc) and solved numerically using the *ode15s* solver. Since we write mole balances for each possible saccharide S_{G_i}, the total number of ODEs depends on the degree of polymerization (DP) distribution of S_{G_i}. For a given S_{G_i} distribution, a total of $5 + DP_{max}$ ODEs are required, where DP_{max} is the maximum DP of a given cellulosic substrate. Parameters listed in Table S1 were used for initial modeling work; at later stages we experimentally measured certain parameters, and also performed a simple regression analysis to estimate parameters from experimental data (Table S3). Initial conditions (C_{Ec}, $C_{Tr,v}$, $C_{Tr,s}$, I, and S_{G_i} at t_0) were chosen to be representative of typical experimental conditions. We approximate $S_{G_i}(t_0)$ with a log-normal distribution, which agrees qualitatively well with experimental data (e.g. see [13]):

$$S_{G_i}(t_0) = \overline{C} f\left(\log i; \overline{DP}, \sigma_{DP}^2\right) \tag{S106}$$

$$= \frac{\overline{C}}{c_{v,DP}\overline{DP}\sqrt{2\pi}} e^{-\frac{1}{2}\left(\frac{\log i - \overline{DP}}{c_{v,DP}\overline{DP}}\right)^2} \tag{S107}$$

where $f\left(\log i; \overline{DP}, \sigma_{DP}^2\right)$ is the probability density function of the normal distribution, $\overline{C} = \sum_{i>4} S_{G_i}$ is total cellulose (mM), i is DP (number of glucose monomers), $\overline{DP}$ is mean DP, and $c_{v,DP}$ is the coefficient of variation of $\overline{DP}$ (with $\sigma_{DP} = c_{v,DP}\overline{DP}$).

We empirically discovered that certain isobutanol toxicity functions ($K^I_{Ec,S_{G_1}}$ and K^I_{Tr}; equations S48 and S42, respectively) resulted in excessively long execution times for *ode15s* and other MATLAB ODE solvers. To make model analysis tractable, we tested the effect of different isobutanol toxicity functions on execution time. Exponential models were found to dramatically improve execution time:

$$K^I_{Ec,S_{G_1}} = e^{-\frac{I}{I_{Ec,*}}} \tag{S108}$$

and

$$K^I_{Tr} = e^{-\frac{I}{I_{Tr,*}}} \tag{S109}$$

where $I_{Ec,*}$ and $I_{Tr,*}$ are isobutanol inhibition constants (g-iButOH/L) for *E. coli* and *T. reesei*, respectively, and other terms are as described previously. The prior models for $K^I_{Ec,S_{G_1}}$ and K^I_{Tr} offer a better fit to experimental toxicity data, however the exponential models are still suitable for qualitative model analysis, as they reflect monotonically declining growth rate with isobutanol concentration.

2.2 Global sensitivity analysis of TrEc consortium model

We performed a global sensitivity analysis on the TrEc consortium model to map parameter space to consortium performance metrics, identify key parameters controlling consortium behavior, and quantify how parameter uncertainty affects model outputs. We applied the sensitivity analysis strategy proposed in [14], which we describe here briefly. The TrEc consortium model was numerically integrated with 1000 different sets of parameter values sampled from appropriate statistical distributions using latin hypercube selection (LHS) [14]. In addition to parameter values, we also examined the effects of initial conditions (ICs), including microbial biomass concentration and composition, soluble saccharide concentrations, and polysaccharide concentrations and distributions (e.g. $\overline{DP}$ and $c_{v,DP}$) and isobutanol*concentration. We calculated partial rank correlation coefficients (PRCC) [14] between each parameter or IC and a set of output metrics, including mean *T. reesei* growth rate (R_{Tr}; g/L/h), *T. reesei* titer ($C_{Tr}(t_f)$; g/L), mean *E. coli* growth rate (R_{Ec}; g/L/h), *E. coli* titer ($C_{Ec}(t_f)$; g/L), mean cellulose hydrolysis rate (R_{Cel}; g/L/h), *E. coli* population fraction at fermentation endpoint ($X_{Ec}(t_f)$; g/g-total microbial biomass), fraction of substrate carbon consumed by *E. coli* ($P_{C\to Ec}$; g/g-total), isobutanol yield ($Y_{I/S}$; g/g-cellulose), isobutanol titer ($I(t_f)$; g/L), and isobutanol productivity (Q_I; g/g-cellulose/h).

LHS is a stratified sampling-without-replacement technique, where random parameter distributions are divided into N equally probable intervals, which are then sampled [14]. To explore the entire parameter range, each interval for each parameter is sampled exactly once without replacement [14]. A matrix is generated that consists of N rows corresponding to the sample size (i.e. total number of parameter sets), and of k columns corresponding to the total number of varied parameters [14]. Parameter and IC values were sampled from either a normal distribution or uniform distribution. For a normal distribution:

$$a_{i,j} = F^{-1}\left(p_{i,j}; \mu_j, (c_{v,j}\mu_j)\right) \tag{S110}$$

where $a_{i,j}$ is the value of parameter j in LHS sample i, $F^{-1}\left(p_{i,j}; \mu_j, (c_{v,j}\mu_j)\right)$ is the normal inverse cumulative distribution function, $p_{i,j}$ is the LHS probability for parameter j in sample i, μ_j is the mean value of parameter j, and $c_{v,j}$ is the coefficient of variation for parameter j (with $\sigma = c_{v,j}\mu_j$). For a uniform distribution:

*For certain processing schemes initial isobutanol concentration may be non-zero (i.e. residual isobutanol in repeated-batch fermentations)

$$a_{i,j} = a_{j,min} + p_{i,j}\,(a_{j,max} - a_{j,min}) \tag{S111}$$

where $a_{j,min}$ is the lower bound on parameter j, $a_{j,max}$ is the upper bound of parameter j, and other terms are as described above.

For parameters that can be arbitrarily varied (i.e. ICs) or that have a wide range of equally probable values, we sampled from a uniform distribution; all other parameters were sampled from a normal distribution. Table S1 contains a list of all investigated parameters, sampling distribution (normal or uniform) for each parameter, and values of μ_j / $c_{v,j}$ or $a_{j,min}$ / $a_{j,max}$.

The TrEc consortium model was numerically integrated with each set of sampled parameter values and ICs, and the above output metrics (R_{Tr}, $C_{Tr}(t_f)$, R_{Ec}, $C_{Ec}(t_f)$, R_{Cel}, X_{Ec}, $P_{C->Ec}$, $Y_{I/S}$, $I(t_f)$, and Q_I) were calculated. LHS sampling and numerical integration were performed with MATLAB. We performed this analysis on a high-performance computing cluster (4 cores total; 2.67 GHz Intel Xeon X5650 processors; 4 GB RAM/core). Partial Rank Correlation Coefficients (PRCC) were calculated by rank transforming parameters and outputs, and then calculating partial correlation coefficients between each parameter and model output [14]. PRCC represents a robust correlation metric for nonlinear but monotonic relationships between model inputs (parameters) and outputs, as long as minimal correlation exists between the inputs [14]. Parameter PRCCs are shown with hierarchical clustering (Wards method; Euclidean distance) in Fig S2; statistically insignificant PRCCs ($p < 0.05$) are set to 0.

2.3 Local sensitivity analysis of estimated RUTC30/NV3 parameter set

To identify parameters/ICs that could be adjusted to improve performance, we conducted a local sensitivity analysis on the RUTC30/NV3 parameter/IC set (estimated via regression to experimental data; Table S3). The TrEc consortium model was numerically integrated with one-at-a-time $\pm 25\%$ perturbations to each parameter/IC. Effects of parameter perturbations were quantified by response coefficients, defined as $\Delta Z\%/|\Delta X\%|$, where $\Delta Z\%$ is % change in output Z and $\Delta X\%$ is % change in parameter X. Response coefficients were calculated for the following outputs: mean *T. reesei* growth rate (R_{Tr}; g/L/h), *T. reesei* titer ($C_{Tr}(t_f)$; g/L), mean *E. coli* growth rate (R_{Ec}; g/L/h), *E. coli* titer ($C_{Ec}(t_f)$; g/L), mean cellulose hydrolysis rate (R_{Cel}; g/L/h), *E. coli* population fraction at fermentation endpoint ($X_{Ec}(t_f)$; g/g-total microbial biomass), fraction of substrate carbon consumed by *E. coli* ($P_{C\rightarrow Ec}$; g/g-total), isobutanol yield ($Y_{I/S}$; g/g-cellulose), isobutanol titer ($I(t_f)$; g/L), and isobutanol productivity (Q_I; g/g-cellulose/h). Response coefficients for $Y_{I/S}$ and R_{cel} are shown for top 10 parameters (ranked by $Y_{I/S}$) in Fig 2E in the main text.

2.4 Theoretical analysis of isobutanol production with TrEc consortium model

To simulate and analyze isobutanol production by the TrEc consortium, we numerically integrated the TrEc consortium model over a range $X_{Ec}(t_0)$ values using *E. coli* parameter values and ICs corresponding to point denoted by white * in Fig 1C, with F_a modified to 0.011; see Table S2 for list of parameters/ICs. The selected parameter/IC set represents an optimistic (but realistic) collection of values which give high $Y_{I/S}$ while still maintaining reasonable R_{cel}. For each numerical solution, key fermentation metrics were calculated: mean *T. reesei* growth rate (R_{Tr}; g/L/h), *T. reesei* titer ($C_{Tr}(t_f)$; g/L), mean *E. coli* growth rate (R_{Ec}; g/L/h), *E. coli* titer ($C_{Ec}(t_f)$; g/L), mean cellulose hydrolysis rate (R_{Cel}; g/L/h), *E. coli* population fraction at fermentation endpoint ($X_{Ec}(t_f)$; g/g-total microbial biomass), fraction of substrate carbon consumed by *E. coli* ($P_{C\rightarrow Ec}$; g/g-total), isobutanol yield ($Y_{I/S}$; g/g-cellulose), isobutanol titer ($I(t_f)$; g/L), and isobutanol productivity (Q_I; g/g-cellulose/h). R_{cel}, $Y_{I/S}$, and Q_I vs. $X_{Ec}(t_0)$ are shown in Fig 1D, while $I(t_f)$ vs. $X_{Ec}(t_0)$ is shown in Fig S3A.

2.5 Regression of model to experimental data

We performed a simple regression of the TrEc consortium model to experimental data obtained from the *T. reesei* RUTC30 monoculture on 20 g/L MCC, *T. reesei* RUTC30 / *E. coli* K12 bi-culture on 10 g/L MCC, and *T. reesei* RUTC30 / *E. coli* NV3 pSA55/69 bi-culture on 20 g/L MCC. We attempted to fit experimentally measured insoluble cellulose concentration (gDW/L), *T. reesei* RUTC30 biomass concentration (gDW/L), *E. coli* biomass concentration (gDW/L), and isobutanol concentration (for RUTC30/NV3 bi-cultures; g/L) to model predictions. For each variable,

crude fit was evaluated as the residual sum of squares over all time points: $RSS = \sum_{t=t_0}^{t_f} \left(y_{exp}(t) - y_{model}(t)\right)^2$, where $y_{exp}(t)$ the is experimental value at time t and $y_{model}(t)$ is the predicted value. Regression was performed by manually adjusting model parameters to minimize RSS for each variable, using initial parameter values from literature (Table S1), in-house monoculture experiments (shown in Table S3), and, for RUTC30/NV3 bi-cultures, estimates based on mass balances of NV3 fermentation products (Table S8).

For the *T. reesei* RUTC30 monoculture, reasonable fit between experimental data and modeling predictions was obtained by adjusting a single parameter, $Y_{S_{G_1}/C_{Tr}}$ (Table S3). Obtaining reasonable fits for the RUTC30/K12 bi-culture required adjusting $\mu_{max,Tr,S_{G_1}}$, $K_{Tr,S_{G_1}}$, and $Y_{S_{G_1}}/C_{Tr}$ for *T. reesei* and $\mu_{max,Ec,S_{G_1}}$, $k_{Ec,d}$, $K_{Ec,S_{G_1}}$, $Y_{S_{G_1}}/C_{Ec}$, and $m_{Ec,S_{G_1}}$ for *E. coli* (Table S3). In addition to cellulose and microbial biomass, we also quantified total protein, exoglucanase, endoglucanase, β-glucosidase, glucose, and cellobiose concentrations in the RUTC30/K12 bi-culture and attempted to fit our model to experimentally measured values; attaining reasonable fit required adjusting $Y_{E_T/C_{Tr}}$, k_{E_T}, k_{EG1}, k_{CBHI}, k_{CBH2}, k_{BGL,G_2}, k_{BGL,G_3}, and k_{BGL,G_4} (Table S3).

For the RUTC30/NV3 bi-culture, regression of model to experimental data required adjusting $\mu_{max,Tr,S_{G_1}}$, $k_{Tr,d}$, $K_{Tr,S_{G_1}}$, $Y_{S_{G_1}}/C_{Tr}$, $k_{v\to s}$, m_{Tr}, $I_{Tr,*}$, k_{E_T}, and $Y_{E_T/C_{Tr}}$ for *T. reesei* and $\mu_{max,Ec,S_{G_1}}$, $k_{Ec,d}$, $K_{Ec,S_{G_1}}$, $Y_{S_{G_1}}/C_{Ec}$, $m_{Ec,S_{G_1}}$, $Y^{growth}_{I/S_{G_1}}$, and $Y^{maint}_{I/S_{G_1}}$ for *E. coli* (Table S3). Initial estimates for $Y_{S_{G_1}}/C_{Tr}$, m_{Tr}, $Y_{S_{G_1}}/C_{Ec}$, $m_{Ec,S_{G_1}}$, $Y^{growth}_{I/S_{G_1}}$, and $Y^{maint}_{I/S_{G_1}}$ were calculated via mass balance of primary *E. coli* NV3 pSA55/69 fermentation products (described below in *Materials and methods*; values given in Table S8).

2.6 Steady state analysis of simplified TrEc model

2.6.1 Criteria for steady state population composition

The system of ODEs for the simplified TrEc consortium model does not have a non-trivial steady-state. However, we can consider the case of a pseudo-steady state in which microbial population composition is fixed:

$$\frac{d}{dt}\left(\frac{C_{Ec}}{C_{Tr}}\right) = 0 \tag{S112}$$

Simplifying and rearranging:

$$\frac{1}{C_{Ec}}\frac{dC_{Ec}}{dt} - \frac{1}{C_{Tr}}\frac{dC_{Tr}}{dt} = 0 \tag{S113}$$

...

$$\frac{\mu_{max,Ec}S_{G_1}}{K_{S,Ec} + S_{G_1}} = \frac{\mu_{max,Tr}\left(S_{G_1} + \theta_{G_2\to G_1}S_{G_2}\right)}{K_{S,Tr} + S_{G_1} + \theta_{G_2\to G_1}S_{G_2}} \tag{S114}$$

This pseudo-steady state can be satisfied if S_{G_2} and S_{G_1} are constant:

$$\frac{dS_{G_2}}{dt} = r^{cel}_{S_{G_2}} - r^{BGL}_{S_{G_2}} = 0 \tag{S115}$$

$$= \frac{k_{cel}E_{cel}S_C}{K_{M,cel} + S_C} - \frac{k_{BGL}E_{BGL}S_{G_2}}{K_{M,BGL} + S_{G_2}} = 0 \tag{S116}$$

and

$$\frac{dS_{G_1}}{dt} = r^{BGL}_{S_{G_1}} - r^{Ec}_{S_{G_1}} - r^{Tr}_{S_{G_1}} = 0 \tag{S117}$$

$$= \frac{k_{BGL}E_{BGL}S_{G_2}}{K_{M,BGL} + S_{G_2}} - Y_{S_{G_1}/C_{Ec}}\frac{\mu_{max,Ec}S_{G_1}}{K_{S,Ec} + S_{G_1}}C_{Ec} - Y_{S_{G_1}/C_{Tr}}\frac{\mu_{max,Tr}\left(S_{G_1} + \theta_{G_2\to G_1}S_{G_2}\right)}{K_{S,Tr} + S_{G_1} + \theta_{G_2\to G_1}S_{G_2}}C_{Tr} = 0 \tag{S118}$$

The above expressions cannot be satisfied since C_{Ec} , C_{Tr}, E_{cel}, E_{BGL}, and S_C are all potentially changing with time. We can make a simplifying assumption that for all times $S_C \gg K_{M,cel}$, making it possible for the system to reach a pseudo-steady state. Physically, this could be interpreted as having an unlimited cellulose supply, or alternately that the TrEc consortium is serial passaged before cellulose becomes limiting. Assuming $S_C \gg K_{M,cel}$, substituting $E_{cel} = Y_{E_{cel}/C_{Tr}} C_{Tr}$, $E_{BGL} = Y_{E_{BGL}/C_{Tr}} C_{Tr}$, $C_{Ec} = X\left(C_{Ec} + C_{Tr}\right)$, and $C_{Tr} = (1-X)\left(C_{Ec} + C_{Tr}\right)$ (where X is *E. coli* population fraction; g-*E. coli*/g-total), we can further simplify:

$$\frac{dS_{G_2}}{dt} = k_{cel} Y_{E_{cel}/C_{Tr}} (1-X) - \frac{k_{BGL} Y_{E_{BGL}/C_{Tr}} (1-X) S_{G_2}}{K_{M,BGL} + S_{G_2}} = 0 \tag{S119}$$

and

$$\begin{aligned}\frac{dS_{G_1}}{dt} =& \frac{k_{BGL} Y_{E_{BGL}/C_{Tr}} (1-X) S_{G_2}}{K_{M,BGL} + S_{G_2}} - Y_{S_{G_1}/C_{Ec}} \frac{\mu_{max,Ec} S_{G_1}}{K_{S,Ec} + S_{G_1}} X \\ & - Y_{S_{G_1}/C_{Tr}} \frac{\mu_{max,Tr}\left(S_{G_1} + \theta_{G_2 \to G_1} S_{G_2}\right)}{K_{S,Tr} + S_{G_1} + \theta_{G_2 \to G_1} S_{G_2}} (1-X) = 0\end{aligned} \tag{S120}$$

Note that $\frac{d}{dt}\left(\frac{C_{Ec}}{C_{Tr}}\right) = 0$ implies that X is constant. The three criteria for steady-state population composition are then:

Criterion 1: Constant population fraction

$$\frac{\mu_{max,Ec} S_{G_1}}{K_{S,Ec} + S_{G_1}} = \frac{\mu_{max,Tr}\left(S_{G_1} + \theta S_{G_2}\right)}{K_{S,Tr} + S_{G_1} + \theta S_{G_2}} \tag{S121}$$

Criterion 2: Constant cellobiose concentration

$$k_{cel} Y_{E_{cel}/C_{Tr}} - \frac{k_{BGL} Y_{E_{BGL}/C_{Tr}} S_{G_2}}{K_{M,BGL} + S_{G_2}} = 0 \tag{S122}$$

Criterion 3: Constant glucose concentration

$$\begin{aligned}&\frac{k_{BGL} Y_{E_{BGL}/C_{Tr}} (1-X) S_{G_2}}{K_{M,BGL} + S_{G_2}} - Y_{S_{G_1}/C_{Ec}} \frac{\mu_{max,Ec} S_{G_1}}{K_{S,Ec} + S_{G_1}} X \\ &- Y_{S_{G_1}/C_{Tr}} \frac{\mu_{max,Tr}\left(S_{G_1} + \theta_{G_2 \to G_1} S_{G_2}\right)}{K_{S,Tr} + S_{G_1} + \theta_{G_2 \to G_1} S_{G_2}} (1-X) = 0\end{aligned} \tag{S123}$$

The steady-state criteria constitute a system of three equations with three unknown variables (X, S_{G_2}, S_{G_1}) that can be solved with analytical or numerical methods.

2.6.2 Non-dimensionalization and analytical solution

To facilitate analysis, we can simplify the above steady-state criteria by non-dimensionalizing the variables. We start with criterion 2, the simplest of the above expressions. Applying $K_{S,Tr}$ as the characteristic cellobiose concentration scale:

$$k_{cel} Y_{E_{cel}/C_{Tr}} - \frac{k_{BGL} Y_{E_{BGL}/C_{Tr}} S_2^*}{K_{BGL}^* + S_2^*} = 0 \tag{S124}$$

where $S_2^* = S_{G_2}/K_{S,Tr}$ and $K_{BGL}^* = K_{M,BGL}/K_{S,Tr}$. This expression can be readily solved for S_2^*:

$$S_2^* = \frac{K_{BGL}^*}{\alpha - 1} \tag{S125}$$

$$\alpha = Y_{BGL/cel} \frac{k_{BGL}}{k_{cel}} \tag{S126}$$

$$Y_{BGL/cel} = Y_{E_{BGL}/C_{Tr}} / Y_{E_{cel}/C_{Tr}} \tag{S127}$$

As would be intuitively expected, the steady-state cellobiose concentration is thus purely a function of cellulase and β-glucosidase kinetics and the relative proportion of these two enzymes. The dimensionless term α describes the relative ratio of β-glucosidase activity to cellulase activity.

Applying $K_{S,Tr}$ as the characteristic glucose and cellobiose concentration scale and $\mu_{max,Tr}$ as the characteristic time scale to criterion 1 yields:

$$\mu^*_{Ec} = \frac{\mu^* S_1}{K^*_S + S^*_1} = \mu^*_{Tr} = \frac{S^*_1 + \theta_{G_2 \to G_1} S^*_2}{1 + S^*_1 + \theta_{G_2 \to G_1} S^*_2} \tag{S128}$$

where $S^*_1 = S_{G_1}/K_{S,Tr}$, $K^*_S = K_{S,Ec}/K_{S,Tr}$, $\mu^* = \mu_{max,Ec}/\mu_{max,Tr}$, and other terms are as described previously. Solving for S^*_1 yields:

$$S^*_1 = \frac{-b \pm \sqrt{b^2 - 4ac}}{2a} \tag{S129}$$

where $a = \mu^* - 1$, $b = \mu^* (1 + \theta_{G_2 \to G_1} S^*_2) - \theta_{G_2 \to G_1} S^*_2 - K^*_S$, $c = -\theta_{G_2 \to G_1} S^*_2 K^*_S$, and other terms are as described previously. The physically meaningful root(s) of the above equation satisfy $0 \leq S^*_1 < \infty$. With expressions for S^*_1 and S^*_2, we can solve criterion 3 for X. We first apply the above dimensional scalings to criterion 3 and divide by $Y_{S_{G_1}/C_{Tr}}$ to yield:

$$\begin{aligned} \frac{k_{BGL} Y_{E_{BGL}/S_{G_1}} S^*_2}{\mu_{max,Tr} (K^*_{BGL} + S^*_2)} (1 - X) - Y_{Tr/Ec} \frac{\mu^* S^*_1}{K^*_S + S^*_1} X \\ - \frac{S^*_1 + \theta_{G_2 \to G_1} S^*_2}{1 + S^*_1 + \theta_{G_2 \to G_1} S^*_2} (1 - X) = 0 \end{aligned} \tag{S130}$$

where $Y_{E_{BGL}/S_{G_1}} = Y_{E_{BGL}/C_{Tr}}/Y_{S_{G_1}/C_{Tr}}$ and $Y_{Tr/Ec} = Y_{S_{G_1}/C_{Ec}}/Y_{S_{G_1}/C_{Tr}}$. Solving for X and simplifying yields:

$$X = \frac{\mu^*_{Tr} - \beta r^*_{BGL}}{\mu^*_{Tr} - Y_{Tr/Ec} \mu^*_{Ec} - \beta r^*_{BGL}} \tag{S131}$$

where:

$$\mu^*_{Tr} = \frac{S^*_1 + \theta_{G_2 \to G_1} S^*_2}{1 + S^*_1 + \theta_{G_2 \to G_1} S^*_2} \tag{S132}$$

$$\mu^*_{Ec} = \frac{\mu^* S^*_1}{K^*_S + S^*_1} \tag{S133}$$

$$r^*_{BGL} = \frac{S^*_2}{K^*_{BGL} + S^*_2} \tag{S134}$$

$$\beta = \frac{k_{BGL} Y_{BGL/S_{G_1}}}{\mu_{max,Tr}} \tag{S135}$$

The μ^*_{Tr} term represents dimensionless *T. reesei* growth rate, μ^*_{Ec} is dimensionless *E. coli* growth rate, and βr^*_{BGL} is a dimensionless ratio of cellobiose hydrolysis rate to glucose uptake rate by *T. reesei*. $X > 0$ requires that $\mu^* > Y_{Tr/Ec} \mu^* + \beta r^*_{BGL}$.

A summary of dimensionless parameters derived in this section can be found in Table S4.

Steady state carbon flow partition can be calculated as:

$$P_{C \to Ec} = \frac{Y_{Tr/Ec} \mu^*_{Ec} X}{Y_{Tr/Ec} \mu^*_{Ec} X + \mu^*_{Tr} (1 - X)} \tag{S136}$$

where $P_{C \to Ec}$ is the ratio of glucose uptake by *E. coli* to total microbial glucose uptake.

2.7 Numerical analysis of simplified TrEc model

For dynamic analysis, the ODEs for the simplified TrEc consortium model (Equations S91-S105; section 1.8) were implemented in MATLAB and solved numerically with $ode15s$, using parameter values as indicated (described in Table S4&S5, and figure captions).

Adding isobutanol production (Equation S103) and toxicity (Equation S104) to our modeling framework makes it impossible for batch cultures to reach non-trivial pseudo-steady states, due to accumulation of isobutanol in the system. Thus we can cannot apply the steady state analysis described above. Instead, we conducted a numerical analysis of the ODE model wherein we simulated iterative serial cultures. This scheme is analogous to repeated batch fermentation, where a fraction of the previous batch is used as inoculum for new batches (Fig S8C, inset). For our theoretical analysis, this was simulated by numerically integrating the ODE system to a fixed endpoint, dividing endpoint variable values by a dilution factor (typically 50 fold), and using these values as initial conditions (ICs) for the next iteration (Fig S8C, inset).

3 Materials and methods

3.1 Media

E. coli strains were propagated in NG50 media [15], supplemented with antibiotics for *E. coli* NV3 pSA55/69 (100 μg/mL ampicillin and 30 μg/mL kanamycin). *T. reesei* monocultures and *T. reesei* / *E. coli* bi-cultures were grown in *Trichoderma* minimal media (TMM) formulated as follows (all concentrations in g/L unless otherwise noted): urea, 1; $(NH_4)_2SO_4$, 4; KH_2PO_4, 6.59; K_2HPO_4, 1.15; $FeSO_4$*$7H_2O$, 0.005; $MnSO_4$*H_2O, 0.0016; $ZnSO_4$*$7H_2O$, 0.0014; $CoCl_2$*$6H_2O$, 0.002; $MgSO_4$, 0.6; $CaCl_2$, 0.6; Tween-80, 0.0186% (v/v); carbon source (glucose, cellobiose, microcrystalline cellulose, or AFEX pre-treated corn stover) as indicated. Antibiotics were added to *E. coli* NV3 pSA55/69 co-cultures as per above, with 0.1 mM IPTG added for induction. For flask culture experiments, TMM was buffered with 0.1M maleate-NaOH at indicated pH [16]; K_2HPO_4 was eliminated and KH_2PO_4 reduced to 1.2 g/L. LB agar [17] was used for *E. coli* cell counting.

3.2 Preparation of inoculum cultures

E. coli was inoculated from cryostock into NG50 medium (with appropriate antibiotics) and incubated at 30°C with agitation until saturated. Cultures were then inoculated 1:100 (by volume) into TMM with 20 g/L glucose and incubated for a further 48 hours at 30°C with agitation. To remove residual glucose, cultures were washed by centrifuging at 18,500 g x 2 minutes, resuspending in TMM without carbon source, and then repeating centrifugation/resuspension. *T. reesei* RUTC30 cryopreserved conidia were inoculated into TMM with 20 g/L glucose and incubated at 30°C with agitation for 48 hours. Cultures were then inoculated 1:50 (by volume) into TMM with indicated carbon source (microcrystalline cellulose or AFEX pre-treated corn stover) and incubated for a further 48 hours at 30°C with agitation.

3.3 Experimental measurement of μ_{max}

μ_{max} (maximum specific growth rate; 1/h) was measured for *E. coli* K12, *E. coli* NV3 pSA55/69, and *T. reesei* RUTC30, under conditions representative of co-culture experiments (glucose TMM media; growth temperature 30°C). μ_{max} was determined by fitting growth data to an exponential model ($\ln C = \ln C_0 + \mu_{max} t$; C is cell density at time t and C_0 is initial density). *E. coli* cell density was determined by measuring optical density at 600 nm (OD_{600}); *T. reesei* cell density was determined via gravimetric analysis (described in section 3.6.1; gDW/L). Growth data was obtained by inoculating cultures in 20 g/L glucose TMM and measuring cell density over time intervals corresponding to the exponential growth phase. *E. coli* growth studies were conducted in microplates. Standard 96-well microplates were filled with 200 μL medium per well and seeded with 2 μL of prepared inoculum culture (described in preceding section) per well. OD_{600} was measured every 10 minutes for 48 to 96 hours using a Spectramax M5 or Versamax plate reader (Molecular Devices, LLC), with 30 °C incubation temperature and agitation between reads. For *T. reesei*, we conducted growth studies using 1 L flask cultures. Flasks were filled with 200 mL medium, seeded with 2 mL prepared inoculum culture, and then incubated at 30 °C with agitation. Triplicate 10 mL samples were taken for gravimetric

dry mass analysis 12, 28, 21, 24, and 27 hours after inoculation. Experimentally measured μ_{max} values are reported in Table S3.

3.4 Characterization of isobutanol toxicity

To characterize isobutanol toxicity in *E. coli* and *T. reesei*, μ_{max} was measured in media spiked with isobutanol at various concentrations, using procedure described in preceding section. To prevent evaporation of isobutanol from cultures, microplates (*E. coli*) were sealed with an impermeable and optically clear adhesive film; flasks (*T. reesei*) were sealed with screw caps and tightly wrapped with parafilm (sterilized with 70% v/v ethanol). μ_{max} values for *E. coli* and *T. reesei* at various isobutanol concentrations are reported in Table S3.

3.5 Experimental measurement of K_S, $Y_{S/C}$, and m

3.5.1 Overview

Modeling and experimental results demonstrate that both growth rates and soluble saccharide (i.e. glucose and cellulose oligosaccharide) concentrations are low in *T. reesei* / *E. coli* bi-cultures on cellulosic substrates, in contrast to saturated growth rates and high glucose concentrations in batch monoculture experiments. Since $K_{S_{G_1}}$ (Monod glucose affinity; g/L) is considered an extant kinetic parameter [18], it should be measured under conditions similar to the co-culture environment. We thus chose to measure $K_{S_{G_1}}$, $Y_{S_{G_1}/C}$ (glucose/biomass yield coefficient; g-glucose/g-biomass), and $m_{S_{G_1}}$ (maintenance coefficient; g-glucose/g-biomass/h) with chemostat experiments; growth rate and substrate concentrations can be precisely controlled via dilution rate, allowing us to simulate bi-culture conditions. Chemostat cultures can reach a steady state in which cell densities and substrate concentrations are constant [1]:

$$\frac{dC}{dt} = 0 \tag{S137}$$

$$\frac{dS_{G_1}}{dt} = 0 \tag{S138}$$

$$\mu = D \tag{S139}$$

where C is cell density, μ is specific growth rate (1/h) and D is dilution rate (media flow rate / culture volume), and other terms are similar to those described above. For single substrate (i.e. glucose) growth, we model μ as

$$\mu = \left(\left(\mu, max, S_{G_1} + \frac{m_{S_{G_1}}}{Y_{S_{G_1}/C}} \right) \frac{S_{G_1}}{K_{S_{G_1}} + S_{G_1}} - \frac{m_{S_{G_1}}}{Y_{S_{G_1}/C}} \right) \tag{S140}$$

where all terms are similar to those described in section 1.7. We can then apply the above steady-state criteria to derive relations for expressions for $K_{S_{G_1}}$, $Y_{S_{G_1}/C}$, and $m_{S_{G_1}}$ in chemostat cultures:

$$K_{S_{G_1}} = \frac{\left(\mu_{max,S_{G_1}} - D\right) S_{G_1}}{D} \tag{S141}$$

and

$$Y^{app}_{S_{G_1}/C} = \frac{S_{G_1,0} - S_{G_1}}{C} \tag{S142}$$

$$= Y_{S_{G_1}/C} + \frac{m_{S_{G_1}}}{D} \tag{S143}$$

where $Y^{app}_{S_{G_1}/C}$ is the apparent yield coefficient (g-glucose/g-cells), $S_{G_1,0}$ is glucose concentration in the chemostat feed (g/L) and other terms are as described previously.

3.5.2 Chemostat experiments

Chemostat studies were conducted in a BioFlo 3000 bioreactor (New Brunswick Scientific), using 1.5 L, 2 L, or 2.5 L culture volumes. Glucose TMM media was used in all studies, with 4 g/L glucose for *T. reesei* cultures and 0.3 g/L glucose for *E. coli* cultures; concentrations were chosen to guarantee that glucose would be the sole limiting nutrient (estimated from data collected during μ_{max} characterization experiments). Bioreactor was maintained at pH 6, temperature 30°C, agitation 200 rpm (dual six blade Rushton impellers; 75 mm diameter), and air flow at 2 vvm (volume air per volume culture per minute) for all studies. Chemostat studies for *E. coli* were performed at dilution rates of $D = 0.04$, 0.063, 0.069, 0.116, 0.174, 0.25, and 0.35 1/h; for *T. reesei*, experiments were performed at $D = 0.019$ and 0.04 1/h. Chemostat studies were initiated by adding prepared inoculum to bioreactor at 1:100 (*E. coli*) or 1:50 (*T. reesei*) volume ratio, and pre-culturing in batch mode for 48 hours. After 48 hours, chemostat mode was started by setting the media feed pump to produce desired dilution rate D; a level probe was used to control the harvest pump rate and thus maintain constant culture volume. Sigma antifoam 204 was added as needed, with 0.02% (v/v) added per supplementation. Samples were taken in triplicate one to two times per turnover period (D^{-1}; h). *E. coli* cultures were analyzed for OD_{600}, viable cell concentration (cells/L), total dry biomass (gravimetric analysis; gDW/L), and glucose (g/L), as per procedures described below; *T. reesei* cultures were analyzed for total dry biomass (gravimetric analysis; gDW/L) and glucose (g/L). Glucose analysis samples were prepared by dispensing culture directly from the bioreactor into syringes filled with steel beads chilled at -20°C and then filtering through 0.22 μm membranes to sterilize; this procedure quenches microbial metabolism, ensuring accurate measurement of low residual glucose concentrations [19]. Steady state was assumed when biomass and glucose concentrations stabilized to constant values (within error limits) for two to three consecutive samples. After taking steady-state samples, feed pump was adjusted to next desired dilution rate and sampling was continued. To avoid adaptive evolution, chemostat experiments were run for < 15 turnovers. $K_{S_{G_1}}$ was calculated from D, glucose concentration (S_{G_1}), and μ_{max}. To determine $Y_{S_{G_1}/C}$ and $m_{S_{G_1}}$, we collected data at various values of D and performed a linear regression of $1/D$ against $Y^{app}_{S_{G_1}/C}$, taking $Y_{S_{G_1}/C}$ as the y-intercept and $m_{S_{G_1}}$ as the slope. Values of $K_{S_{G_1}}$, $Y_{S_{G_1}/C}$, and $m_{S_{G_1}}$ determined from chemostat studies are reported in Table S3.

3.6 Analytical methods

3.6.1 Gravimetric analysis

Flask culture samples 8 to 10 mL culture samples were washed by centrifuging at 18,500 g x 15 minutes, resuspending in 45 mL dH2O, and repeating centrifugation. Cell pellets were transferred to pre-weighed aluminum boats and dried for 24 hours at 70°C; total dry mass was taken as the difference between boat with cell pellet and empty boat weight.

Bioreactor samples Culture samples (40 mL for batch and *E. coli* chemostat cultures; 20 mL for *T. reesei* chemostat cultures) were centrifuged at 18,500 g x 15 minutes and resuspended in 45 mL 20% (w/v) citric acid. Samples were then vortexed for 1 minute and incubated at room temperature for 10 minutes to dissolve phosphate and carbonate precipitates [20]. Samples were washed by centrifuging at 18,500 g x 15 minutes, resuspending in 45 mL dH2O, and repeating centrifugation. Cell pellets were lyophilized at 0.02 millibar / -45°C in pre-weighed tubes; total dry mass was taken as the difference between tube with cell pellet and empty tube weight.

3.6.2 Total secreted protein assay

Total protein concentration in culture supernatant was measured using the Bradford assay as described in [21], with bovine serum albumin (BSA) as a calibration standard. Undiluted, 1:10, $1:10^2$, and $1:10^3$ diluted samples (in 0.15 M NaCl) were analyzed; BSA calibration standards ranged from 0 to 10 μg/mL in assay mix.

3.6.3 β-glucosidase assay

β-glucosidase activity was assayed using p-nitrophenyl-β-D-glucopyranoside (pNPG) as a substrate, using a previously described procedure [22] with modifications. Undiluted, 1:10, and $1:10^2$ diluted culture samples in 50 mM citrate buffer (pH 4.8) were pre-incubated at 50°C for 5 minutes. Reactions were initiated by adding pNPG to 2.5 mM and incubating for 10 minutes at 50°C . Reactions were quenched and color developed by adding NaOH-glycine

buffer (pH 10.8) to 0.2 M. Concentration of released p-nitrophenol was determined by measuring absorbance at 405 nm; p-nitrophenol calibration standards ranged from 0 to 0.25 mM in assay mix. One international unit (IU) of enzyme activity was defined as the amount of enzyme required to produce 1 μmol of p-nitrophenol per minute.

3.6.4 Endoglucanase assay

Endoglucanase activity was assayed using carboxymethylcellulose (CMC) as a substrate, using a previously described procedure [23] with modifications. Undiluted, 1:10, 1:10^2, and 1:10^3 diluted culture samples in 50 mM citrate buffer (pH 4.8) were pre-incubated at 50°C for 5 minutes. Reactions were initiated by adding CMC to 1% (w/v) and incubating for 30 minutes at 50°C. Reactions were quenched and analyzed for reducing sugars by adding one equivalent volume of 3,5-dinitrosalicylic acid (DNS) reagent mix [23] and incubating at 95°C for 5 minutes. Concentration of 3-amino,5-nitrosalicylic acid (produced stoichiometrically from reducing sugars) was determined by measuring absorbance at 540 nm; glucose was used as a calibration standard with 0 to 1.67 mM in assay mix. One international unit (IU) of enzyme activity was defined as the amount of enzyme required to produce 1 μmol glucose-equivalent per minute.

3.6.5 Exoglucanase assay

Exoglucanase activity was assayed using microcrystalline cellulose as a substrate [24], with the procedure otherwise identical to the endoglucanase assay.

3.6.6 Carbohydrate analysis

Carbohydrate analysis of co-culture samples was performed by the Great Lakes Bioenergy Research Center (GLBRC); procedures are described in detail in [25]. Briefly, co-culture samples were washed and lyophilized as described in preceding sections for gravimetric analysis. Lyophilized co-culture material was finely ground and treated with trifluoroacetic acid (TFA) to hydrolyze the hemicellulose / matrix polysaccharide fraction [25]. The resulting soluble saccharides were derivatized to alditol acetates and analyzed via GC/MS [25]. The insoluble fraction remaining after TFA hydrolysis (consisting of crystalline cellulose, lignin, and other recalcitrant components) was analyzed for crystalline cellulose using the Updegraff procedure [25]. Our analysis methods cannot distinguish between carbohydrates originating in lignocellulose and those from microbial biomass (i.e. *T. reesei* and *E. coli*). To account for microbial carbohydrate contributions, we analyzed carbohydrate composition of pure microbial biomass samples (*T. reesei* RUTC30 grown on 20 g/L MCC TMM media; *E. coli* K12 grown on 20 g/L glucose TMM media). Composition data for detectable carbohydrates in microbial biomass and AFEX pre-treated corn stover (AFEX CS) are shown in Table S7. After determining microbial biomass concentrations (described below), we subtracted the microbial contribution to each measured carbohydrate:

$$S_{i,actual} = S_{i,meas} - x_{i,Ec}C_{Ec} - x_{i,Tr}C_{Tr} \tag{S144}$$

where $S_{i,meas}$ is the measured concentration of carbohydrate i (arabinose, xylose, mannose, galactose, hemicellulose dervied glucan, and crystalline cellulose; g/L), $x_{i,Ec}$ is the fraction of i in *E. coli* biomass (g-*i*/g-Ec), $x_{i,Tr}$ is the fraction of i in *T. reesei* biomass (g-*i*/g-Tr), $S_{i,actual}$ is the corrected carbohydrate concentration (g/L), and other terms are as described previously. Uncultivated media samples (MCC or AFEX CS TMM media) were analyzed to determine initial concentration of major carbohydrates, $S_i|_{t_0}$ (g/L); $S_{i,actual}$ and $S_i|_{t_0}$ were used in calculation of conversions, yields, etc.

3.6.7 Estimation of *T. reesei* biomass

Mannose was selected as a biomarker for *T. reesei* biomass; mannose makes up a substantial fraction of total *T. reesei* biomass while being a relatively minor component of *E. coli* and AFEX CS (Table S7). To develop a correlation between *T. reesei* biomass and mannose, *T. reesei* RUTC30 was cultured on 20 g/L MCC TMM media and samples were taken periodically for carbohydrate analysis. *T. reesei* fraction of total dry mass (X_{Tr}; g/g-total) was found to be linear with mannose fraction of total mass (X_{mann}; g/g-total), with $X_{Tr} = 15.02X_{mann} + 0.1173$ ($R^2 = 0.88$; $\sigma_{est} = 0.07$); results shown in Fig S9. *T. reesei* biomass concentration (g/L) is calculated as $C_{Tr} = X_{Tr}C_{Tot}$, where terms are as described above.

3.6.8 Estimation of *E. coli* biomass and plasmid maintenance

E. coli biomass was estimated by cell counting (direct measurement of viable cell concentration) or via subtractive mass balance (indirect measurement of total cell concentration). For cell counting, 10 fold serial dilutions of culture samples were prepared and 100 μL aliquots plated onto LB agar; to determine pSA55/69 cell counts, LB agar was supplemented with 100 μg/mL ampicillin and 30 μg/mL kanamycin. Plates were incubated at 37°C overnight and counted, using two to four plating replicates. An estimated cell mass of $1.5 \pm 0.3x10^{-13}$ g/cell for *E. coli* K12 and $8.9 \pm 0.3x10^{-13}$ g/cell for *E. coli* NV3 pSA55/69 (determined from chemostat and co-culture experimental data) was used to convert cells/L to gDW/L. For *E. coli* NV3 pSA55/69 cultures, the fraction of cells retaining pSA55/69 was taken as fraction of amp^R / kan^R cells out of total cells. To estimate *E. coli* biomass via mass balance, we write a total mass balance on insoluble co-culture components and solve for *E. coli* biomass concentration:

$$C_{Ec} = \frac{C_{Tot} - \sum S_{i,meas} - (1 - \sum x_{i,Tr})\, C_{Tr} - C_{res}}{1 - \sum x_{i,Ec}} \tag{S145}$$

where C_{Tot} is the total dry mass concentration (gDW/L), C_{res} is the residual insoluble fraction (i.e. undegraded lignin, etc; g/L), and the other terms are as defined previously.

3.6.9 Quantification of soluble saccharides and fermentation products

Isobutanol and soluble saccharide concentrations (> 50 mg/L) were quantified using high performance liquid chromatography (HPLC). Culture samples were incubated at 99°C for 10 minutes to thermally denature enzymes, and then filtered through a 0.22 μm membrane. Samples were then analyzed on an Agilent 1100 HPLC equipped with a Rezex ROA ion-exchange column, using 5 μL injection volume, 60°C column temperature, 0.005N H_2SO_4 mobile phase at 0.5 mL/min, and a refractive index detector (RID) for analyte quantification. Soluble saccharide concentrations in the range from 5 to 50 mg/L were quantified using hexokinase-based assays. Glucose was quantified with a D-Glucose HK kit (Megazyme Internatonal, cat #K-GLUHK) following manufacturer's protocol, but with reagent and sample volumes scaled down by a factor of 10. Oligosaccharide concentrations were measured via enzymatic hydrolysis to glucose and subsequent glucose quantification. Oligosaccharides were hydrolyzed by combining samples with an equivalent volume of 2 IU/mL *A. niger* β-glucosidase (Megazyme International) in 0.1 M acetate buffer (pH 4) and incubating at 49°C for 20 minutes. Samples were neutralized with 1 M NaOH and then assayed for glucose as described above. For chemostat studies, where glucose concentrations ranged < 5 mg/L, glucose was quantified using a fluorometric glucose assay kit (BioVision, cat #K606) following manufacturers protocol; depleted chemostat media was used as a blank and for preparation of calibration standards.

3.6.10 Identification of unknown fermentation products

HPLC analysis of *T. reesei* RUTC30 / *E. coli* NV3 pSA55/69 bi-cultures revealed numerous fermentation products. The four most abundant products have retention times (RT) of 15.4, 19.1, 26.3, and 39 minutes, collectively representing $> 75\%$ of the total peak area. We identified and quantified these products by running calibration standards for candidate compounds; candidates were selected on basis of expected fermentation products and a manufacturer-supplied RT index for the Aminex HPX-87H column (equivalent to Rezex ROA column; US/EG Bulletin 1847, Bio-rad) . The RT 15.4, 19.1, 26.3, and 39 min peaks were subsequently identified as succinate, acetate, ethanol, and isobutanol, respectively.

3.6.11 Estimate of substrate partition via mass balance on *E. coli* NV3 pSA55/69 fermentation products

We estimated substrate partition between *T. reesei* RUTC30 and *E. coli* NV3 pSA55/69 in bi-culture by performing a mass balance on primary NV3 pSA55/69 fermentation products (isobutanol, ethanol, acetate, and succinate). To the best of our knowledge, these fermentation products are unique to NV3 pSA55/69 and were not observed in *T. reesei* monocultures[†]. For each fermentation product j, the glucose G consumed to form product j was calculated based on the theoretical yield coefficient $Y_{j/G}$ (g-product j / g-glucose): $C_{G,j} = C_j / Y_{j/G}$, where $C_{G,j}$ and C_j are glucose and product concentrations, respectively. Total substrate consumed to form fermentation products was then calculated as $\sum C_{G,j}$. **Since this estimate does not include CO_2 or minor, unidentified fermentation products, it represents a**

[†]Even under anoxic conditions, *T. reesei* does not produce anaerobic metabolites (i.e. ethanol, acetate, glycerol, etc.) [26]

lower bound on substrate consumption by NV3 pSA55/69. Total substrate consumption by *T. reesei* was calculated by subtracting estimated substrate consumed by NV3 pSA55/69 from total substrate consumed. Glucose-biomass yield coefficients, maintenance coefficients, and isobutanol yield coefficients were then calculated based on estimated substrate consumption, and are given in Table S8.

4 Supporting figures and tables

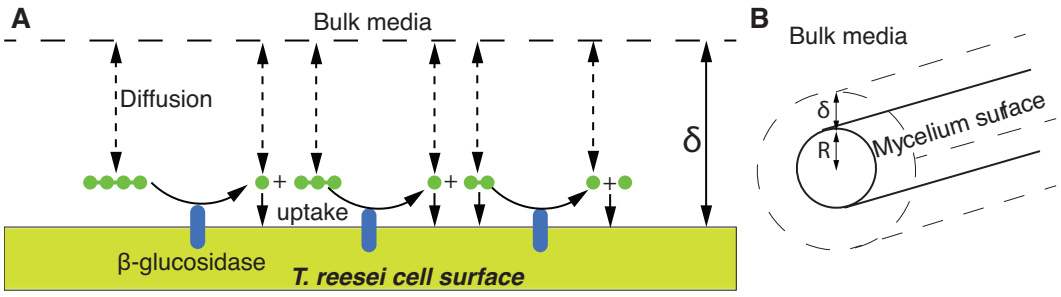

Fig. S1. Mass transfer model for oligosaccharide hydrolysis by cell-wall bound β-glucosidase of *T. reesei*. (A) Hydrolysis and diffusion of oligosaccharides at *T. reesei* cell surface **(B)** Approximation of mycelium as cylindrical surface.

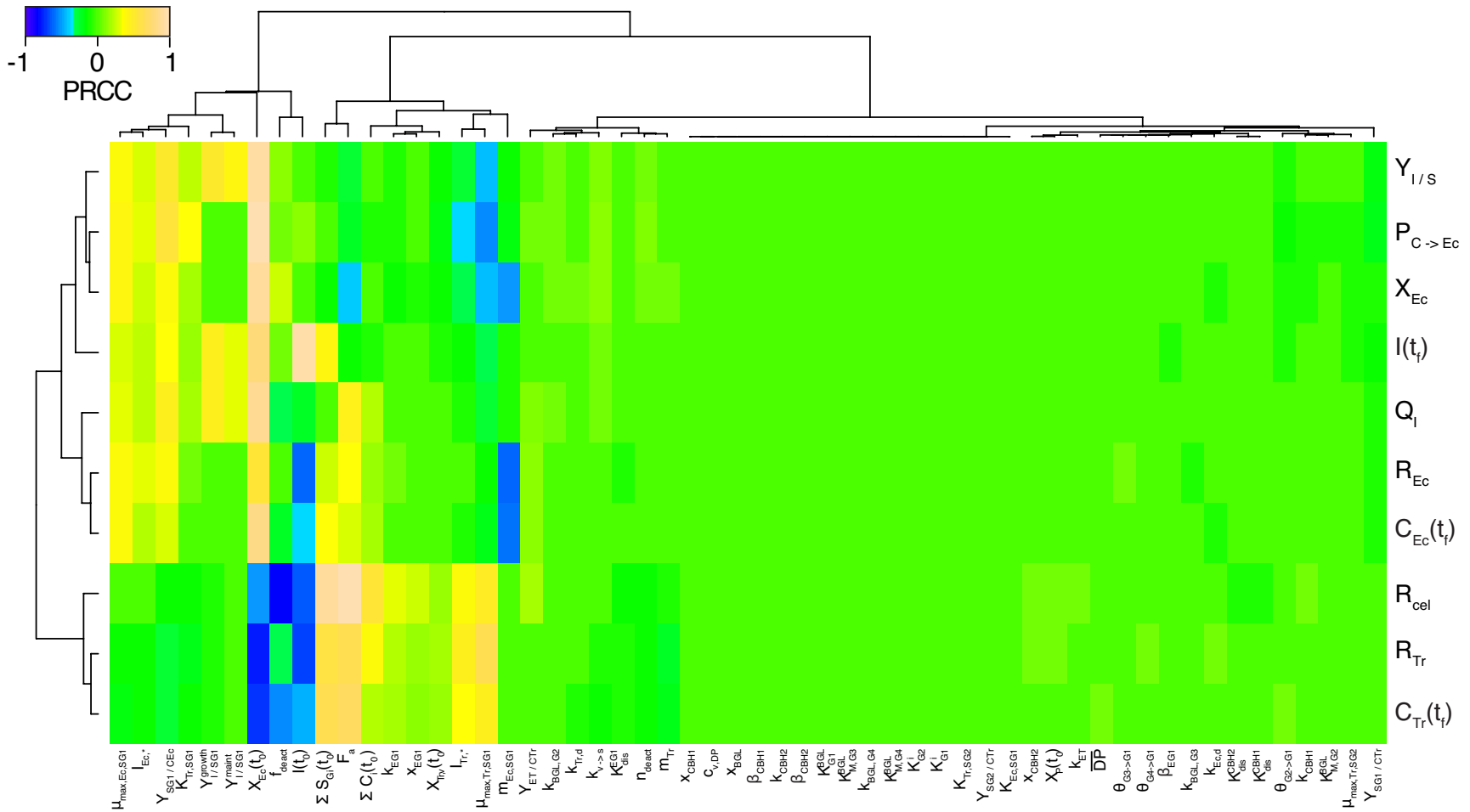

Fig. S2. Global sensitivity analysis of TrEC consortium model - full results. The TrEc consortium model was numerically integrated with 1000 different sets of parameter values and initial conditions (ICs) sampled from appropriate statistical distributions using latin hypercube selection (LHS) [14]. We calculated partial rank correlation coefficients (PRCC) [14] between each parameter or IC and a set of output metrics, including mean *T. reesei* growth rate (R_{Tr}; g/L/h), *T. reesei* titer ($C_{Tr}(t_f)$; g/L), mean *E. coli* growth rate (R_{Ec}; g/L/h), *E. coli* titer ($C_{Ec}(t_f)$; g/L), mean cellulose hydrolysis rate (R_{Cel}; g/L/h), *E. coli* population fraction at fermentation endpoint ($X_{Ec}(t_f)$; g/g-total microbial biomass), fraction of substrate carbon consumed by *E. coli* ($P_{C \to Ec}$; g/g-total), isobutanol yield ($Y_{I/S}$; g/g-cellulose), isobutanol titer ($I(t_f)$; g/L), and isobutanol productivity (Q_I; g/g-cellulose/h). Parameter PRCCs are shown with hierarchical clustering (Wards method; Euclidean distance); statistically insignificant PRCCs ($p < 0.05$) set to 0. For description of parameters, parameter values, and statistical distributions used, see Table S1.

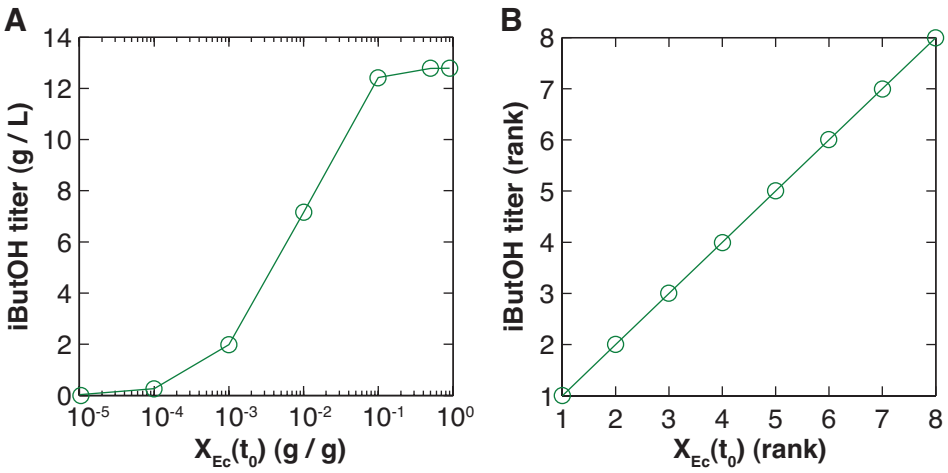

Fig. S3. Model predictions for isobutanol production. Model solutions were found using parameter values and ICs corresponding to point denoted by white * in Fig 1C (values listed in Table S2). **(A)** Predicted isobutanol titer vs. $X_{Ec}(t_0)$. **(B)** Rank transform of data in panel A (i.e. isobutanol titer rank vs. $X_{Ec}(t_0)$ rank); $R^2 = 1$. See Fig 1D for R_{cel}, $Y_{I/S}$, and Q_I vs. $X_{Ec}(t_0)$.

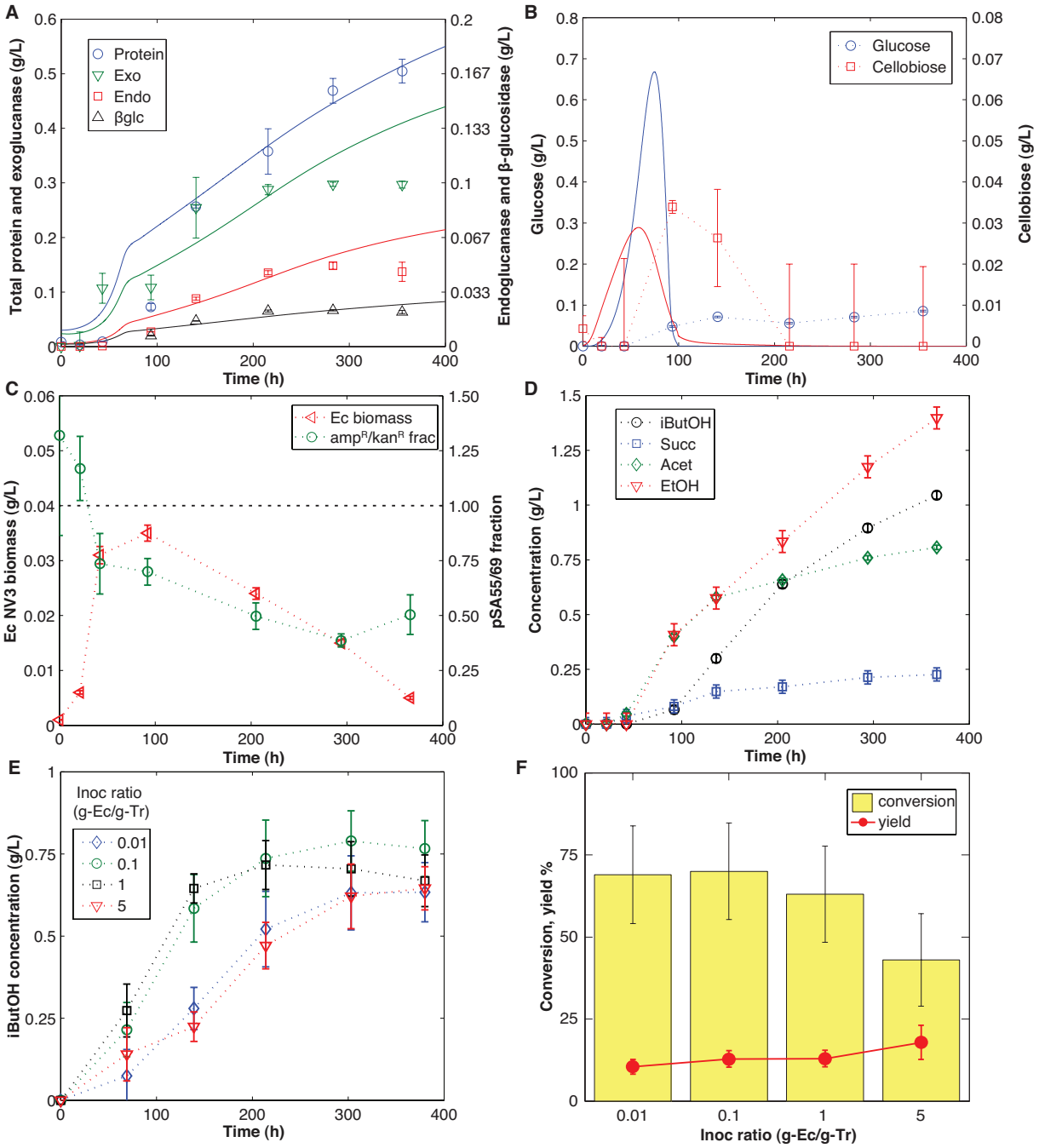

Fig. S4. Additional results for RUTC30/K12 and RUTC30/NV3 bi-cultures on microcrystalline cellulose (MCC). **(A)** Total protein (Protein), exoglucanase (Exo), endoglucanase (Endo), and β-glucosidase (βglc) concentrations for RUTC30/K12 bi-culture on 10 g/L MCC (corresponding to Fig 2B). Model predictions shown as smooth lines, with experimental data points. Error bars are $\pm$SD for $N = 3$ technical replicates. **(B)** Glucose and cellobiose concentrations for RUTC30/K12 bi-culture (corresponding to Fig 2B). Model predictions shown as smooth lines, with experimental data points connected with dashed lines. Error bars are $\pm$SD for $N = 3$ technical replicates. **(C)** *E. coli* NV3 biomass and amp^R/kan^R fraction of population (i.e. pSA55/69 fraction) for RUTC30/NV3 bi-culture on 20 g/L MCC (corresponding to Fig 2C). Error bars are $\pm$SD for $N = 2$ to 4 technical replicates. **(D)** Fermentation product concentrations in RUTC30/NV3 bi-culture (corresponding to Fig 2C). Abbreviations: isobutanol, iButOH; ethanol, EtOH; acetate, Acet; succinate, Succ. Error bars are $\pm\sigma_{est}$ from calibration curves. **(E)** Isobutanol production in RUTC30/NV3 bi-cultures inoculated over a series of Ec:Tr ratios on 20 g/L MCC. Error bars are $\pm$SD for $N = 2$ biological replicates. **(F)** Conversion (% MCC consumed) and isobutanol yield (g/g-MCC) for bi-cultures in panel E. Error bars are $\pm$SD for $N = 2$ biological replicates with $N = 3$ technical replicates each.

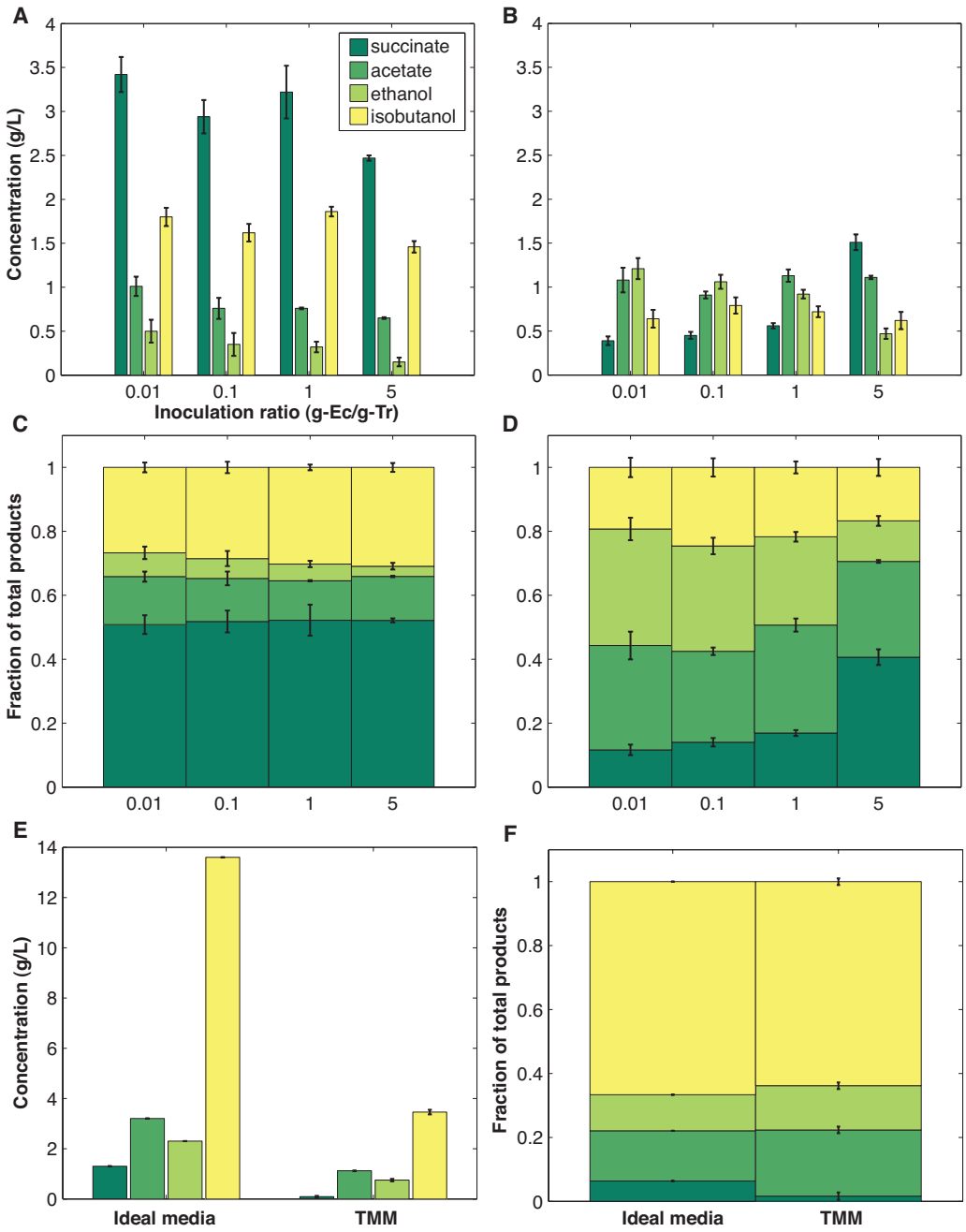

Fig. S5. Endpoint concentrations and relative proportions of major fermentation products in *T. reesei* RUT-C30 / *E. coli* NV3 pSA55/69 bi-cultures on AFEX pre-treated corn stover or MCC, and in monocultures of *E. coli* NV3 pSA55/69 on glucose. Error bars are $\pm$SD for $N = 2$ biological replicates. Endpoint concentrations in bi-cultures: **(A)** 20 g/L AFEX pre-treated corn stover and **(B)** 20 g/L MCC. Relative fermentation product proportions in bi-cultures: **(C)** 20 g/L AFEX pre-treated corn stover and **(D)** 20 g/L MCC. **(E)** Endpoint concentrations in *E. coli* NV3 pSA55/69 monocultures on glucose. Data for monocultures on both TMM media and ideal conditions (yeast-extract supplemented media / glucose feeding) are shown; data for ideal conditions adapted from [27]. **(F)** Relative fermentation product proportions in *E. coli* NV3 pSA55/69 monocultures.

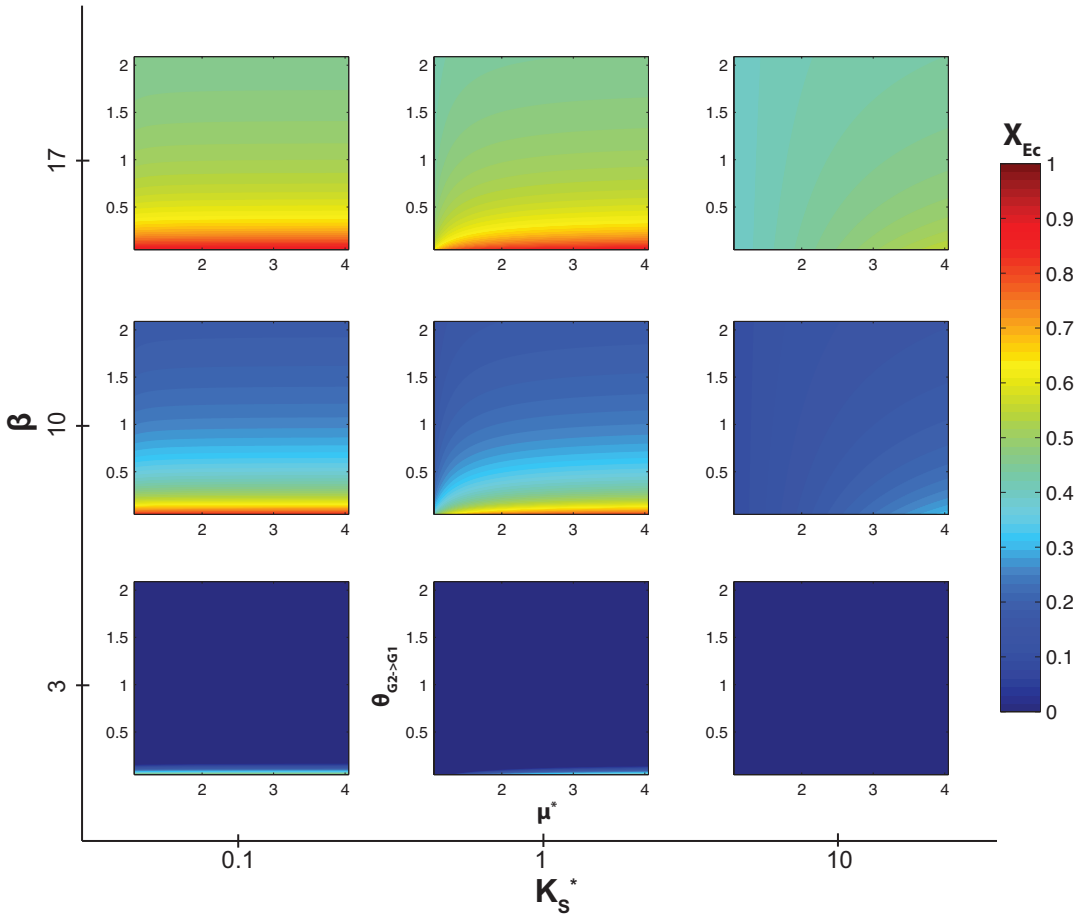

Fig. S6. Steady state analysis of simplified TrEc model: X_{Ec} (*E. coli* population fraction) as a function of β, K_S^*, μ^*, and $\theta_{G_2 \to G_1}$ over biologically reasonable ranges for each parameter. Parameter values are as follows: $\alpha = 8.7$, $K_{BGL}^* = 23.25$, $Y_{Tr/Ec} = 1.5$; $\beta = 3, 10, 17$, $K_S^* = 0.1, 1, 10$, $\mu^* = 1.05...4.05$, and $\theta_{G_2 \to G_1} = 0.05...2.05$. For explanation of parameters see section 1.8.

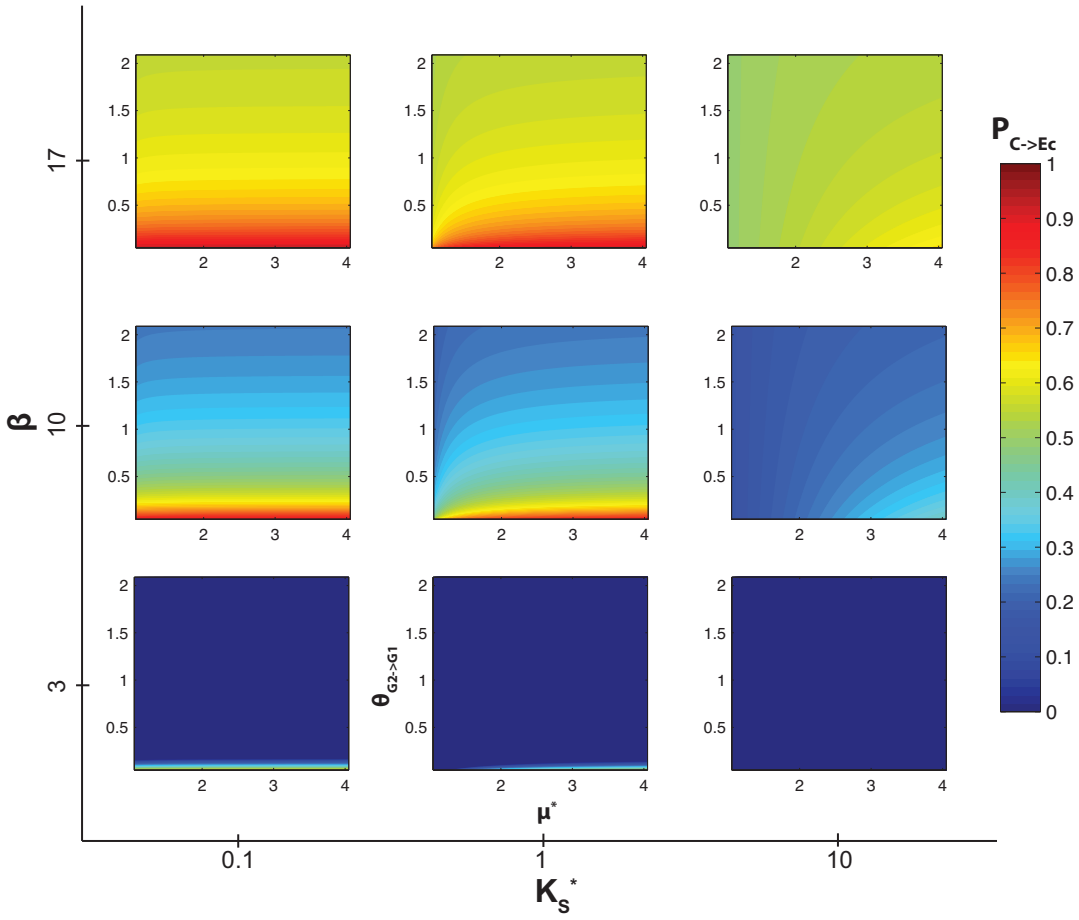

Fig. S7. Steady state analysis of simplified TrEc model: $P_{C\rightarrow Ec}$ (carbon flow partition to *E. coli*) as a function of β, K_S^*, μ^*, and $\theta_{G_2\rightarrow G_1}$ over biologically reasonable ranges for each parameter. Parameter values are as follows: $\alpha = 8.7$, $K_{BGL}^* = 23.25$, $Y_{Tr/Ec} = 1.5$; $\beta = 3, 10, 17$, $K_S^* = 0.1, 1, 10$, $\mu^* = 1.05...4.05$, and $\theta_{G_2\rightarrow G_1} = 0.05...2.05$. For explanation of parameters see section 1.8.

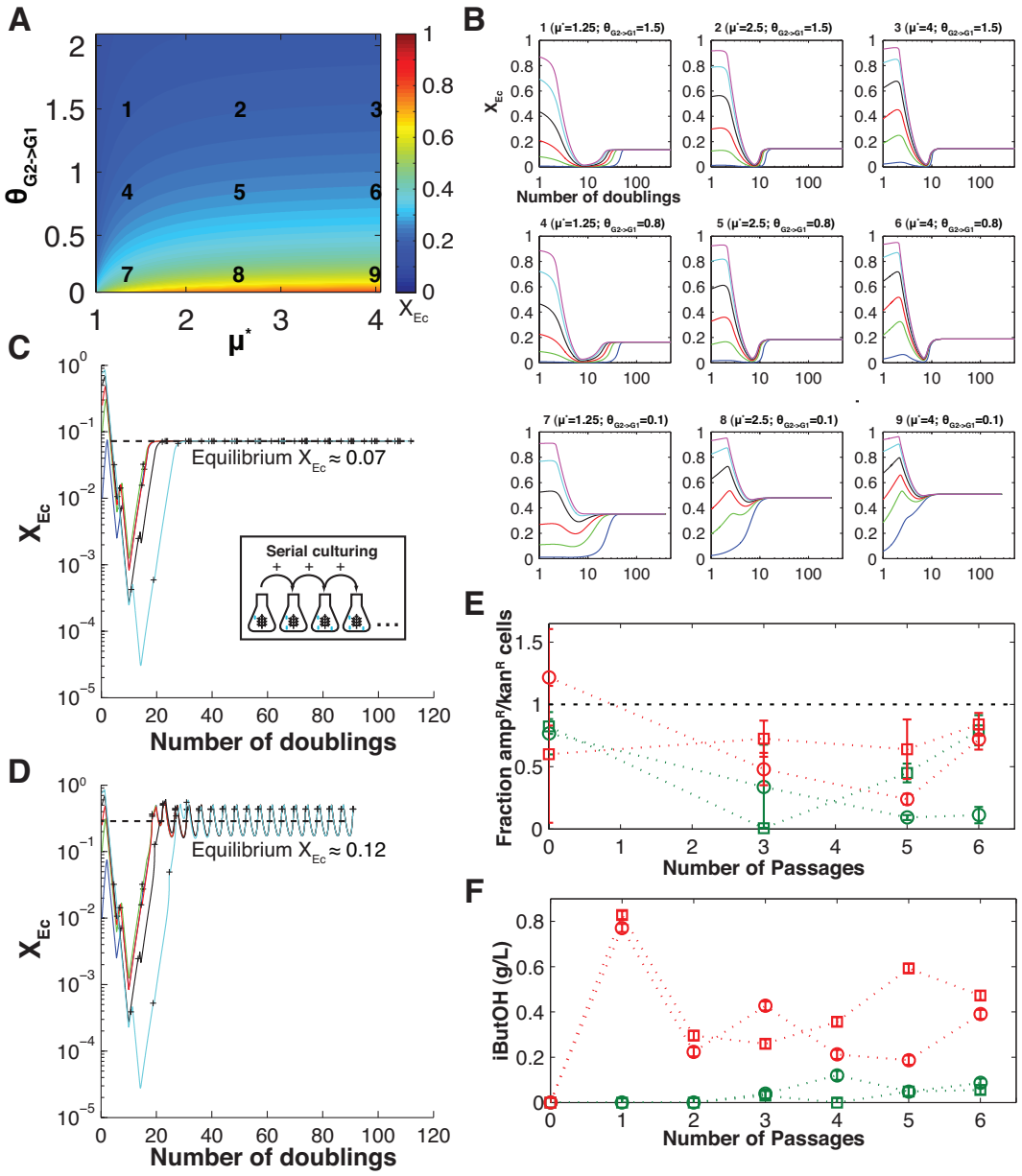

Fig. S8. Additional modeling and experimental results for cooperator-cheater dynamics in the TrEc consortium. **(A)** Steady state population composition (X_{Ec}; *E. coli* population fraction) calculated as a function of μ^* and $\theta_{G_2 \to G_1}$, with $\alpha = 8.7$, $K^*_{BGL} = 23.25$, $Y_{Tr/Ec} = 1.5$, and $\beta = 10$. **(B)** Numerical ODE solutions corresponding to μ^* and $\theta_{G_2 \to G_1}$ values at each labeled point in panel A. For each μ^*, $\theta_{G_2 \to G_1}$ point, ODEs were solved with various initial X_{Ec} values. For explanation of parameters see section 1.8 and Table S4. **(C)** Numerical ODE solutions over a range of $X_{Ec}(t_0)$ values for parameter set corresponding to RUTC30/NV3 bi-cultures, with $Y_{I/S_{G_1}} = 0$ (i.e. no isobutanol production/toxicity). Inset depicts serial culturing scheme used in numerical simulations, with "+" indicating passaging points. Parameter values were estimated using *E. coli* monoculture data presented in [8] and [27], and are as follows: $\mu^* = 1.61$, $\theta_{G_2 \to G_1} = 1.7$, $K^*_S = 0.05$, $\alpha = 8.7$, $K^*_{BGL} = 23.25$, $Y_{Tr/Ec} = 3.15$, and $\beta = 40$. **(D)** Numerical ODE solutions over a range of $X_{Ec}(t_0)$ values, with $Y_{I/S_{G_1}} = 0.25$ g-isobutanol/g-glucose, isobutanol toxicity parameters as given in Table S5, and all remaining parameters the same as panel C. **(E)** amp^R/kan^R fraction (i.e. pSA55/69 fraction) of *E. coli* NV3 populations in RUTC30/NV3 serial bi-cultures (corresponding to Fig 4D). **(F)** Isobutanol concentrations in RUTC30/NV3 serial bi-cultures (corresponding to Fig 4D).

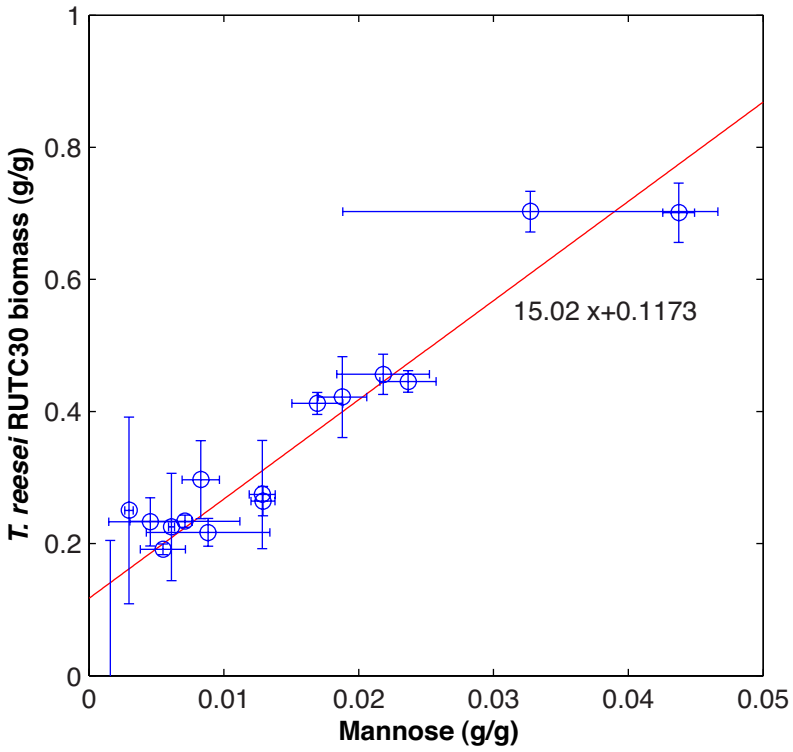

Fig. S9. Correlation between *T. reesei* RUTC30 biomass and mannose. *T. reesei* RUTC30 was cultured on 20 g/L MCC TMM media and samples were taken periodically for carbohydrate analysis. *T. reesei* mass fraction (i.e. non-cellulose fraction; g/g-total) shown as a function of mannose mass fraction (g/g-total); $R^2 = 0.88$ and $\sigma_{est} = 0.07$ for linear regression. Error bars are $\pm$SD for $N = 3$ technical replicates; results from two independent experiments (sampled at different time points) shown.

Table S1. List of all parameters used in global sensitivity analysis (Fig 1B). Sampling distribution (normal or uniform), values of μ_j, $c_{v,j}$ (normal distribution) or $a_{j,min}$, $a_{j,max}$ (uniform distribution), description/units, and key notes/references listed for each parameter.

IC or parameter	$\mu_j/a_{j,min}$	$c_{v,j}/a_{j,max}$	Distribution	Description	Notes / source
$\log(F_a)$	-3	-1	Uniform	Fractional accessible bonds	Range from PASC to MCC [9]
$\overline{DP}$	1.6	2.25	Uniform	Cellulose mean degree of polymerization (DP; log scale)	Median value corresponds to MCC [9]
$c_{v,DP}$	0	0.1	Uniform	c_v of cellulose DP distribution	Est. from [13]
$\sum S_{G_i}(t_0)$	10	40	Uniform	Initial cellulose concentration (g/L)	–
$\sum C_i(t_0)$	0.1	1	Uniform	Total initial microbial biomass (g/L)	–
$X_{Tr,v}(t_0)$	0.72	0.2	Normal	Initial fraction vegetative mycelium	Biologically reasonable range
$X_P(t_0)$	0.5	0.2	Normal	Initial protein concentration (fraction of total biomass)	–
$\log(X_{Ec})(t_0)$	-3	0	Uniform	Initial Ec population (fraction of total biomass)	–
$I(t_0)$	0	5	Uniform	Initial isobutanol concentration (g/L)	–
x_{CBH1}	0.6	0.2	Normal	Fraction of CBH1 in total protein	[9]
x_{CBH2}	0.2	0.2	Normal	Fraction of CBH2 in total protein	[9]
x_{EG1}	0.12	0.2	Normal	Fraction of EG1 in total protein	[9]
x_{BGL}	0.03	0.2	Normal	Fraction of BGL in total protein	Est. from [28] and [3]
n_{deact}	5	0.2	Normal	Declining substrate reactivity exponent	Est. from [11]
f_{deact}	0.8	0.99	Uniform	$1-f_{deact}$ = residual cellulase activity at 100% conversion	Est. from [11]
k_{EG1}	24	0.2	Normal	EG1 rate constant (mmol/g-EG1/h)	Est. from [9]
K_{dis}^{EG1}	0.33	0.2	Normal	EG1 dissociation constant (mM)	[9]
β_{EG1}	0.166	0.2	Normal	$2\alpha_{EG1}/MW_{EG1}$ (g-EG1/mmol substrate sites)	Est. from [29] and [7]
k_{CBH1}	4.8	0.2	Normal	CBH1 rate constant (mmol/g-CBH1/h)	Est. from [9]
K_{dis}^{CBH1}	0.25	0.2	Normal	CBH1 dissociation constant (mM)	[9]
β_{CBH1}	0.019	0.2	Normal	$1/MW_{CBH1}$ (g-CBH1/mmol)	Est. from [29] and [7]
k_{CBH2}	9.6	0.2	Normal	CBH2 rate constant (mmol/g-CBH2/h)	Est. from [9]
K_{dis}^{CBH2}	0.25	0.2	Normal	CBH2 dissociation constant (mM)	[9]
β_{CBH2}	0.022	0.2	Normal	$1/MW_{CBH2}$ (g-CBH2/mmol)	Est. from [29] and [7]
k_{BGL,G_2}	339	0.2	Normal	BGL rate constant for cellobiose (mmol/g-BGL/h)	[10]
K_{M,G_2}^{BGL}	1.36	0.2	Normal	BGL affinity for cellobiose (mM)	[10]
$K_{G_1}^{BGL}$	11.33	0.2	Normal	BGL competitive glucose inhibition constant (mM)	[10]
k_{BGL,G_3}	758	0.2	Normal	BGL rate constant for cellotriose (mmol/g-BGL/h)	
K_{M,G_3}^{BGL}	0.2	0.2	Normal	BGL affinity for cellotriose (mM)	[10]
k_{BGL,G_4}	1810	0.2	Normal	BGL rate constant for cellotetraose (mmol/g-BGL/h)	
K_{M,G_4}^{BGL}	0.38	0.2	Normal	BGL affinity for cellotetraose (mM)	[10]
$K_{G_2}^{i}$	17.2	0.2	Normal	Cellulase (EG1, CBH1, CBH2) non-competitive cellobiose inhibition constant (mM)	Est. from [12]
$K_{G_1}^{i}$	66.6	0.2	Normal	Cellulase (EG1, CBH1, CBH2) non-competitive glucose inhibition constant (mM)	Est. from [12]
$k_{Tr,d}$	0.005	0.2	Normal	Death rate of senescent mycelium (1/h)	Est. from [5]
$K_{Tr,S_{G_1}}$	0.02	0.5	Normal	Tr glucose affinity (g/L)	Est. from [30]
$K_{Tr,S_{G_2}}$	0.0001	0.5	Normal	Tr cellobiose affinity (g/L)	Est. from [31]
$\theta_{G_2\to G_1}$	1.7	0.2	Normal	Glucose contribution at mycelium surface due to cellobiose hydrolysis (mM/mM)	Calculated from [32] and [33]
$\theta_{G_3\to G_1}$	2.2	0.2	Normal	Glucose contribution at mycelium surface due to cellotriose hydrolysis (mM/mM)	Calculated from [32] and [33]
$\theta_{G_4\to G_1}$	2.5	0.2	Normal	Glucose contribution at mycelium surface due to cellotetraose hydrolysis (mM/mM)	Calculated from [32] and [33]
$Y_{S_{G_1}/C_{Tr}}$	2	0.2	Normal	Glucose/biomass yield coefficient for Tr (g-glucose/g-biomass	Est. from [30]
$Y_{S_{G_2}/C_{Tr}}$	2	0.2	Normal	Cellobiose/biomass yield coefficient for Tr (g-cellobiose/g-biomass)	Est. ≈glucose
$Y_{E_T/C_{Tr}}$	0.5	0.2	Normal	Enzyme/biomass yield coefficient for Tr (g-protein/g-biomass)	Est. from [7] and [34]

Table S1. List of all parameters used in global sensitivity analysis (Fig 1B). Sampling distribution (normal or uniform), values of μ_j, $c_{v,j}$ (normal distribution) or $a_{j,min}$, $a_{j,max}$ (uniform distribution), description/units, and key notes/references listed for each parameter.

IC or parameter	$\mu_j / a_{j,min}$	$c_{v,j} / a_{j,max}$	Distribution	Description	Notes / source
$\mu_{max,Tr,S_{G_1}}$	0.087	0.2	Normal	Maximum specific growth rate of Tr on glucose (1/h)	Est. from [5], [35], and [30]
$\mu_{max,Tr,S_{G_2}}$	0.025	0.5	Normal	Maximum specific growth rate of Tr on cellobiose (1/h)	Est. from [31]
$k_{v\to s}$	0.01	0.2	Normal	Specific rate of conversion of vegetative mycelium to aged mycelium (1/h)	Est. from [5]
m_{Tr}	0.027	0.2	Normal	Maintenance coefficient for Tr (g-substrate/g-biomass/h)	Est. from [30]
$I_{Tr,*}$	2.5	0.2	Normal	Isobutanol inhibition exponent (exponential inhibition model; Eq S109) for Tr (g-iButOH/L)	Est. $\approx 1/2$Ec
k_{E_T}	0.008	0.2	Normal	Specific enzyme production rate of senescent mycelium (g-protein/g-biomass/h)	Est. as $\approx 1/5$ rate of vegetative mycelium
$k_{Ec,d}$	0.001	0.2	Normal	Ec death rate (1/h)	Est. from [36]
$K_{Ec,S_{G_1}}$	0.001	0.5	Normal	Ec glucose affinity (g/L)	Est. from [36]
$Y_{S_{G_1}/C_{Ec}}$	6.4	0.5	Normal	Glucose/biomass yield coefficient for Ec (g-glucose/g-biomass	Est. from [36, 8, 27]
$m_{Ec,S_{G_1}}$	0.23	0.5	Normal	Maintenance coefficient for Ec (g-glucose/g-biomass/h)	Est. from [36, 8, 27]
$\mu_{max,Ec,S_{G_1}}$	0.08	0.2	Normal	Maximum specific growth rate of Ec on glucose (1/h)	Est. from experimental data in this study
$Y^{growth}_{I/S_{G_1}}$	0	0.41	Uniform	Growth associated isobutanol/glucose yield coefficient for Ec (g-iButOH/g-glucose)	Est. from [36, 8, 27]
$Y^{maint}_{I/S_{G_1}}$	0	0.41	Uniform	Maintenance associated isobutanol/glucose yield coefficient for Ec (g-iButOH/g-glucose)	Est. from [36, 8, 27]
$I_{Ec,*}$	5	0.2	Normal	Isobutanol inhibition exponent (exponential inhibition model; Eq S108) for Ec (g-iButOH/L)	Est. from experimental data in this study

Table S2. Parameter/IC set used for Fig 1D

IC or parameter	Value	Notes/Units
$\log(F_a)$	0.011	Fractional accessible bonds
$\overline{DP}$	1.837575	log DP
$c_{v,DP}$	0.07715	c_v for log DP distribution
$\sum S_{G_i}(t_0)$	38.275	g/L
$\sum C_i(t_0)$	0.39295	g/L
$X_{Tr,v}(t_0)$	0.534218988	g/g-Tr
$X_P(t_0)$	0.38759693	g/g-Tr
$\log(X_{Ec})(t_0)$	$-$	Varied
$I(t_0)$	0	g/L
x_{CBH1}	0.550340628	g/g-protein
x_{CBH2}	0.190124743	g/g-protein
x_{EG1}	0.104522697	g/g-protein
x_{BGL}	0.024721558	g/g-protein
n_{deact}	5.056429069	$-$
f_{deact}	0.862985	fraction residual activity
k_{EG1}	19.50465251	mmol/g-EG1/h
K_{dis}^{EG1}	0.432037935	mM
β_{EG1}	0.201202554	g-EG1/mmol substrate sites
k_{CBH1}	5.906670426	mmol/g-CBH1/h
K_{dis}^{CBH1}	0.211643145	mM
β_{CBH1}	0.021438858	g-CBH1/mmol
k_{CBH2}	5.407705866	mmol/g-CBH2/h
K_{dis}^{CBH2}	0.279813116	mM
β_{CBH2}	0.019686308	g-CBH2/mmol
k_{BGL,G_2}	230.3366627	mmol/g-BGL/h
K_{M,G_2}^{BGL}	1.192903359	mM
$K_{G_1}^{BGL}$	11.21350831	mM
k_{BGL,G_3}	819.0841305	mmol/g-BGL/h
K_{M,G_3}^{BGL}	0.204975928	mM
k_{BGL,G_4}	1721.564109	mmol/g-BGL/h
K_{M,G_4}^{BGL}	0.505378801	mM
$K_{G_2}^{i}$	15.55737042	mM
$K_{G_1}^{i}$	57.88640831	mM
$k_{Tr,d}$	0.004948592	1/h
$K_{Tr,S_{G_1}}$	0.02750423	g/L
$K_{Tr,S_{G_2}}$	0.000145105	g/L
$\theta_{G_2 \to G_1}$	1.639599929	mM/mM
$\theta_{G_3 \to G_1}$	2.27368694	mM/mM
$\theta_{G_4 \to G_1}$	1.849122279	mM/mM
$Y_{S_{G_1}/C_{Tr}}$	0.982920472	g-glucose/g-biomass
$Y_{S_{G_2}/C_{Tr}}$	2.204600565	g-cellobiose/g-biomass
$Y_{E_T/C_{Tr}}$	0.563872784	g-protein/g-biomass
$\mu_{max,Tr,S_{G_1}}$	0.065140033	1/h
$\mu_{max,Tr,S_{G_2}}$	0.028999478	1/h
$k_{v \to s}$	0.01211186	1/h
m_{Tr}	0.022947716	g-substrate/g-biomass/h
$I_{Tr,*}$	6.72	g-iButOH/L
k_{E_T}	0.007195281	g-protein/g-biomass/h
$k_{Ec,d}$	0.000839755	1/h
$K_{Ec,S_{G_1}}$	0.001006893	g/L
$Y_{S_{G_1}/C_{Ec}}$	11.4715259	g-glucose/g-biomass

Table S2. Parameter/IC set used for Fig 1D

IC or parameter	Value	Notes/Units
$m_{Ec,S_{G_1}}$	0.142935429	g-glucose/g-biomass/h
$\mu_{max,Ec,S_{G_1}}$	0.080260701	1/h
$Y^{growth}_{I/S_{G_1}}$	0.321645	g-iButOH/g-glucose
$Y^{maint}_{I/S_{G_1}}$	0.408565	g-iButOH/g-glucose
$I_{Ec,*}$	4.86	g-iButOH/L

Table S3. Experimentally measured model parameters. Listed parameters are organized by experiment, denoted by shading: microplate, RUTC30 flask (glucose), chemostat, RUTC30 on MCC, RUTC30/K12 on MCC, and RUTC30/NV3 on MCC. Monoculture data for *E. coli* JCL260 (BW25113/F' [*traD36, proAB+, lacIq ZΔM15*] Δ*adhE*,Δ*frdBC*,Δ*fnr-ldhA*,Δ*pta*, Δ*pflB*) included [8]. *We estimated $\mu_{max,Ec,S_{G_1}}$ for *E. coli* NV3 pSA55/69 by multiplying $\mu_{max,Ec,S_{G_1}}$ for NV3 (i.e. the plasmid free strain) by the ratio of JCL260 pSA55/69 : JCL260 $\mu_{max,Ec,S_{G_1}}$ values.

Species	Experiment notes	Parameter	Value	Units
E. coli K12	Microplate	$\mu_{max,Ec,S_{G_1}}$	0.41 ± 0.02	1/h
E. coli NV3	Microplate	$\mu_{max,Ec,S_{G_1}}$	0.43 ± 0.03	1/h
E. coli JCL260	Microplate	$\mu_{max,Ec,S_{G_1}}$	0.34 ± 0.01	1/h
E. coli NV3 pSA55/69*	Microplate	$\mu_{max,Ec,S_{G_1}}$	0.14 ± 0.02	1/h
E. coli JCL260 pSA55/69	Microplate	$\mu_{max,Ec,S_{G_1}}$	0.11 ± 0.01	1/h
E. coli JCL260 pSA55/69	Microplate; NG50; 0% (w/v) i-BtOH	$\mu_{max,Ec,S_{G_1}}$	0.11 ± 0.005	1/h
E. coli JCL260 pSA55/69	Microplate; NG50; 0.25% (w/v) i-BtOH	$\mu_{max,Ec,S_{G_1}}$	0.071 ± 0.003	1/h
E. coli JCL260 pSA55/69	Microplate; NG50; 0.5% (w/v) i-BtOH	$\mu_{max,Ec,S_{G_1}}$	0.006 ± 0.002	1/h
T. reesei RUTC30	Flask; glucose	$\mu_{max,Tr,S_{G_1}}$	0.092 ± 0.01	1/h
T. reesei RUTC30	Flask; glucose; 0.2% (w/v) i-BtOH	$\mu_{max,Tr,S_{G_1}}$	0.08 ± 0.01	1/h
E. coli K12	Chemostat	$K_{Ec,S_{G_1}}$	0.24 ± 0.19	mg/L
E. coli K12	Chemostat	$Y_{S_{G_1}/C_{Ec}}$	1.4 ± 0.7	g-glucose/g-biomass
E. coli K12	Chemostat	$m_{Ec,S_{G_1}}$	0.4 ± 0.2	g-glucose/g-biomass/h
T. reesei RUTC30	Chemostat	$K_{Tr,S_{G_1}}$	24 ± 18	mg/L
T. reesei RUTC30	Chemostat	$Y_{S_{G_1}/C_{Tr}}$	1.4 ± 0.3	g-glucose/g-biomass
T. reesei RUTC30	Chemostat	m_{Tr}	0.0175 ± 0.005	g-substrate/g-biomass/h
T. reesei RUTC30	RUTC30 on MCC	$Y_{S_{G_1}/C_{Tr}}$	3.95	g-glucose/g-biomass
T. reesei RUTC30	RUTC30/K12 on MCC	$\mu_{max,Tr,S_{G_1}}$	0.08	1/h
T. reesei RUTC30	RUTC30/K12 on MCC	$K_{Tr,S_{G_1}}$	0.1	mg/L
T. reesei RUTC30	RUTC30/K12 on MCC	$Y_{S_{G_1}/C_{Tr}}$	1.75	g-glucose/g-biomass
T. reesei RUTC30	RUTC30/K12 on MCC	$Y_{S_{G_2}/C_{Tr}}$	1.75	g-cellobiose/g-biomass
T. reesei RUTC30	RUTC30/K12 on MCC	$Y_{E_T/C_{Tr}}$	0.1	g-protein/g-biomass
T. reesei RUTC30	RUTC30/K12 on MCC	k_{E_T}	0.001	g-protein/g-biomass/h
Endoglucanase I	RUTC30/K12 on MCC	k_{EG1}	67.2	mmol/g-EG1/h
Cellobiohydrolase I	RUTC30/K12 on MCC	k_{CBH1}	13.44	mmol/g-CBH1/h
Cellobiohydrolase II	RUTC30/K12 on MCC	k_{CBH2}	26.88	mmol/g-CBH2/h
β-glucosidase I	RUTC30/K12 on MCC	k_{BGL,G_2}	949.2	mmol/g-BGL/h
β-glucosidase I	RUTC30/K12 on MCC	k_{BGL,G_3}	2122.4	mmol/g-BGL/h
β-glucosidase I	RUTC30/K12 on MCC	k_{BGL,G_3}	5068	mmol/g-BGL/h
E. coli K12	RUTC30/K12 on MCC	$\mu_{max,Ec,S_{G_1}}$	0.0425	1/h
E. coli K12	RUTC30/K12 on MCC	$k_{Ec,d}$	0.00001	1/h
E. coli K12	RUTC30/K12 on MCC	$K_{Ec,S_{G_1}}$	0.00001	mg/L
E. coli K12	RUTC30/K12 on MCC	$Y_{S_{G_1}/C_{Ec}}$	3	g-glucose/g-biomass
E. coli K12	RUTC30/K12 on MCC	$m_{Ec,S_{G_1}}$	0.02	g-glucose/g-biomass/h
T. reesei RUTC30	RUTC30/NV3 on MCC	$\mu_{max,Tr,S_{G_1}}$	0.1268	1/h
T. reesei RUTC30	RUTC30/NV3 on MCC	$k_{Tr,d}$	0.004	1/h
T. reesei RUTC30	RUTC30/NV3 on MCC	$k_{v\to s}$	0.01	1/h
T. reesei RUTC30	RUTC30/NV3 on MCC	m_{Tr}	0.0081	g-substrate/g-biomass/h
T. reesei RUTC30	RUTC30/NV3 on MCC	$I_{Tr,*}$	0.125	g-iButOH/L
T. reesei RUTC30	RUTC30/NV3 on MCC	$K_{Tr,S_{G_1}}$	15	mg/L
T. reesei RUTC30	RUTC30/NV3 on MCC	$Y_{S_{G_1}/C_{Tr}}$	1.243	g-glucose/g-biomass
T. reesei RUTC30	RUTC30/NV3 on MCC	$Y_{S_{G_2}/C_{Tr}}$	1.243	g-cellobiose/g-biomass
T. reesei RUTC30	RUTC30/NV3 on MCC	k_{E_T}	0.0001	g-protein/g-biomass/h
T. reesei RUTC30	RUTC30/NV3 on MCC	$Y_{E_T/C_{Tr}}$	0.139	g-protein/g-biomass

Table S3. Experimentally measured model parameters. Listed parameters are organized by experiment, denoted by shading: microplate, RUTC30 flask (glucose), chemostat, RUTC30 on MCC, RUTC30/K12 on MCC, and RUTC30/NV3 on MCC. Monoculture data for *E. coli* JCL260 (BW25113/F' [*traD36, proAB+, lacIq ZΔM15*] Δ*adhE,*Δ*frdBC,*Δ*fnr-ldhA,*Δ*pta,* Δ*pflB*) included [8]. *We estimated $\mu_{max,Ec,S_{G_1}}$ for *E. coli* NV3 pSA55/69 by multiplying $\mu_{max,Ec,S_{G_1}}$ for NV3 (i.e. the plasmid free strain) by the ratio of JCL260 pSA55/69 : JCL260 $\mu_{max,Ec,S_{G_1}}$ values.

Species	Experiment notes	Parameter	Value	Units
E. coli NV3 pSA55/69	RUTC30/NV3 on MCC	$\mu_{max,Ec,S_{G_1}}$	0.0858	1/h
E. coli NV3 pSA55/69	RUTC30/NV3 on MCC	$k_{Ec,d}$	0.00525	1/h
E. coli NV3 pSA55/69	RUTC30/NV3 on MCC	$K_{Ec,S_{G_1}}$	0.1	mg/L
E. coli NV3 pSA55/69	RUTC30/NV3 on MCC	$Y_{S_{G_1}}/C_{Ec}$	26.26	g-glucose/g-biomass
E. coli NV3 pSA55/69	RUTC30/NV3 on MCC	$m_{Ec,S_{G_1}}$	1.97	g-glucose/g-biomass/h
E. coli NV3 pSA55/69	RUTC30/NV3 on MCC	$Y^{growth}_{I/S_{G_1}}$	0.025	g-iButOH/g-glucose
E. coli NV3 pSA55/69	RUTC30/NV3 on MCC	$Y^{maint}_{I/S_{G_1}}$	0.1216	g-iButOH/g-glucose

Table S4. Summary of dimensionless parameters in simplified TrEc consortium model. All terms are as described in section 2.6.2. See Table S5 for baseline values for *T. reesei* RUTC30 and *E. coli* K12.

Parameter	Definition	Description
μ^*	$\frac{\mu_{max,Ec}}{\mu_{max,Tr}}$	Ec:Tr growth rate ratio (cheater benefits)
K_S^*	$\frac{K_{S,Ec}}{K_{S,Tr}}$	Ec:Tr glucose affinity ratio (inverse cheater benefits)
$\theta_{G_2 \to G_1}$	$\frac{\Delta S_{G_1}}{S_{G_2}}$	Increase in glucose concentration relative to the bulk medium at the *T. reesei* cell surface due to cellobiose hydrolysis (cooperator privileged access)
$Y_{Tr/Ec}$	$\frac{Y_{S_{G_1}/C_{Ec}}}{Y_{S_{G_1}/C_{Tr}}}$	*T. reesei* biomass-substrate yield coefficient to *E. coli* yield coefficient ratio (relative resource utilization efficiency of cooperator)
β	$\frac{k_{BGL} Y_{BGL/S_{G_1}}}{\mu_{max,Tr}}$	Glucose production rate to *T. reesei* uptake rate ratio (relative resource production/consumption by cooperator)
α	$Y_{BGL/cel} \frac{k_{BGL}}{k_{cel}}$	Cellobiose hydrolysis rate to cellulose hydrolysis rate ratio (relative consumption/production of intermediate substrate)
K_{BGL}^*	$\frac{K_{M,BGL}}{K_{S,Tr}}$	Dimensionless β-glucosidase cellobiose affinity

Table S5. Baseline parameters for *T. reesei* RUTC30 and *E. coli* K12 used in steady state analysis of the simplified TrEc consortium model. Other parameters, including $\theta_{G_2 \to G_1}$, β, $K_{S,Ec}$ (K_S^*) and $\mu_{max,Ec}$ (μ^*) were varied to explore population dynamics and steady state composition. NV3 parameters were estimated from [8] or [27], or were estimated from experimental data via regression (Table S3).

Parameter	Value	Description	Notes and source
$\mu_{max,Tr}$	0.087	Maximum specific growth rate of Tr on glucose (1/h)	Est. from [5], [35], and [30]
$K_{S,Tr}$	0.02	Tr glucose affinity (g/L)	Est from [30]
$Y_{E_{cel}/C_{Tr}}$	0.5	Enzyme/biomass yield coefficient for Tr (g-protein/g-biomass)	Est. from [7] and [34]
$Y_{E_{BGL}/C_{Tr}}$	0.015	β-glucosidase / biomass yield coefficient for Tr (g-BGL/g-biomass)	Est. from [28] and [3]
$Y_{S_{G_1}/C_{Tr}}$	2	Glucose/biomass yield coefficient for Tr (g-glucose/g-biomass)	Est. from [30]
k_{cel}	0.4	Cellulase rate constant (g-cellobiose/g-cellulase/h)	Est. from [7]
k_{BGL}	116	β-glucosidase rate constant (g-glucose/g-β-glucosidase/h)	Est. from [10]
$K_{M,BGL}$	0.465	β-glucosidase affinity for cellobiose (g/L)	Est. from [10]
$Y_{BGL/cel}$	0.03	β-glucosidase fraction of total cellulase; same as x_{BGL} (g/g-total)	Est. from [7] and [34]
α	8.7	$\frac{Y_{E_{BGL}/C_{Tr}} k_{BGL}}{Y_{E_{cel}/C_{Tr}} k_{cel}}$	–
$Y_{Tr/Ec}$	1.5	$Y_{S_{G_1}/C_{Ec}} / Y_{S_{G_1}/C_{Tr}}$	Biologically reasonable value
I_{Tr}^*	5	Inhibitory iButOH concentration for Tr (g/L)	Est. $\approx 1/2$ Ec
I_{Ec}^*	10	Inhibitory iButOH concentration for Ec (g/L)	Est. from experimental data in this study
n_{Tr}	1.5	iButOH inhibition exponent for Tr	Biologically reasonable value
n_{Ec}	1.5	iButOH inhibition exponent for Ec	Biologically reasonable value

Table S6. $\mu_{max,Tr}$, $\mu_{max,Ec}$, and μ^* for *E. coli* K12 and *T. reesei* RUTC30 on 20 g/L glucose TMM media at various pH levels. All $\mu_{max,Ec}$ values were measured experimentally; For *T. reesei*, we measured $\mu_{max,Tr}$ at pH 6 and extrapolated to pH 5.5 and 5.3 using data presented in [37].

pH	$\mu_{max,Tr}$ (1/h)	Source	$\mu_{max,Ec}$ (1/h)	Source	μ^*
5.3	0.104 ± 0.01	Est from [37]	0.09 ± 0.01	This study	0.9 ± 0.1
5.5	0.098 ± 0.01	Est from [37]	0.21 ± 0.03	This study	2.1 ± 0.4
6	0.092 ± 0.01	This study	0.39 ± 0.01	This study	4.2 ± 0.5

Table S7. Carbohydrate composition of microbial biomass and AFEX pre-treated corn stover (taken from AFEX CS TMM media sample). Abbreviations: Arabinose, Ara; Xylose, Xyl; Mannose, Mann; Galactose, Gal; Hemicellulose glucan, Glc; Crystalline cellulose, Cry cel. *Neither *T. reesei* nor *E. coli* are known to produce crystalline cellulose; since the Updegraff assay is non-specific, the measured value probably reflects some other recalcitrant polysaccharide.

	Major carbohydrates (g/g)						
Species	**Ara**	**Xyl**	**Mann**	**Gal**	**Glc**	**Cry cel**	**Total**
T. reesei RUTC30	(1 ± 1)E-3	(5 ± 2)E-3	0.049 ± 0.008	0.021 ± 0.003	0.14 ± 0.02	0	0.21 ± 0.02
E. coli K12	(2 ± 0.4)E-4	(2 ± 0.3)E-4	(2 ± 0.5)E-4	(1 ± 0.2)E-3	0.029 ± 0.001	$0.021 \pm 0.005^*$	0.05 ± 0.005
AFEX CS	0.03 ± 0.002	0.20 ± 0.03	(2.6 ± 0.4)E-3	0.01 ± 0.001	0.034 ± 0.007	0.47 ± 0.04	0.74 ± 0.05

Table S8. Substrate partition and yield/maintenance coefficients estimated via mass balance on *E. coli* NV3 pSA55/69 fermentation products for RUTC30/NV3 bi-culture on 20 g/L MCC. Calculations described in *SI Materials and methods*. Mass balance does not include CO_2 or minor, unidentified fermentation products; therefore these estimates represent upper or lower bounds (as indicated).

Species	Parameter	Value	Description	Units	Bound
–	$P_{C->Ec}$	0.39 ± 0.07	fraction of substrate consumed by *E. coli*	g/g-total	Lower
T. reesei RUTC30	$Y_{S_{G_1}}/C_{Tr}$	3.3 ± 1.8	Glucose/biomass yield coefficient for Tr	g-glucose/g-biomass	Upper
T. reesei RUTC30	m_{Tr}	0.013 ± 0.001	Maintenance coefficient for Tr	g-substrate/g-biomass/h	Upper
E. coli NV3 pSA55/69	$Y_{S_{G_1}}/C_{Ec}$	40.4 ± 3.6	Glucose/biomass yield coefficient for Ec	g-glucose/g-biomass	Lower
E. coli NV3 pSA55/69	$m_{Ec,S_{G_1}}$	0.767 ± 0.002	Maintenance coefficient for Ec	g-substrate/g-biomass/h	Lower
E. coli NV3 pSA55/69	$Y^{growth}_{I/S_{G_1}}$	0 ± 0.001	Growth associated isobutanol/glucose yield	g-iButOH/g-glucose	Upper
E. coli NV3 pSA55/69	$Y^{maint}_{I/S_{G_1}}$	0.166 ± 0.004	Maintenance associated isobutanol/glucose yield	g-iButOH/g-glucose	Upper

References

[1] Fogler HS (2006) *Elements of chemical reaction engineering*, (Prentice Hall PTR, Upper Saddle River, NJ), 4th edition.

[2] Lendenmann U, Egli T (1998) Kinetic models for the growth of *Escherichia coli* with mixtures of sugars under carbon-limited conditions. *Biotechnol Bioeng* 59:99–107.

[3] Kubicek CP (1981) Release of carboxymethyl-cellulase and β-glucosidase from cell walls of *Trichoderma reesei*. *Appl Microbiol Biotechnol* 13:226–231.

[4] Gore J, Youk H, van Oudenaarden A (2009) Snowdrift game dynamics and facultative cheating in yeast. *Nature* 459:253–256.

[5] Bader J, Klingspohn U, Bellgardt KH, Schügerl K (1993) Modelling and simulation of the growth and enzyme production of *Trichoderma reesei* Rut C30. *J Biotechnol* 29:121–135.

[6] Mach RL, Strauss J, Zeilinger S, Schindler M, Kubicek CP (1996) Carbon catabolite repression of xylanase I (*xyn1*) gene expression in *Trichoderma reesei*. *Mol Microbiol* 21:1273–1281.

[7] Lynd LR, Weimer PJ, van Zyl WH, Pretorius IS (2002) Microbial cellulose utilization: fundamentals and biotechnology. *Microbiol Mol Biol Rev* 66:506–577.

[8] Atsumi S, Hanai T, Liao JC (2008) Non-fermentative pathways for synthesis of branched-chain higher alcohols as biofuels. *Nature* 451:86–89.

[9] Zhang YH, Lynd LR (2006) A functionally based model for hydrolysis of cellulose by fungal cellulase. *Biotechnol Bioeng* 94:888–898.

[10] Schmid G, Wandrey C (1989) Characterization of a cellodextrin glucohydrolase with soluble oligomeric substrates: experimental results and modeling of concentration-time-course data. *Biotechnol Bioeng* 33:1445–1460.

[11] South CR, Hogsett DAL, Lynd LR (1995) Modeling simultaneous saccharification and fermentation of lignocellulose to ethanol in batch and continuous reactors. *Enzyme Microb Tech* 17:797–803.

[12] Peri S, Karra S, Lee YY, Karim MN (2007) Modeling intrinsic kinetics of enzymatic cellulose hydrolysis. *Biotechnol Prog* 23:626–637.

[13] Mittal A, Katahira R, Himmel ME, Johnson DK (2011) Effects of alkaline or liquid-ammonia treatment on crystalline cellulose: changes in crystalline structure and effects on enzymatic digestibility. *Biotechnol Biofuels* 4:41.

[14] Marino S, Hogue IB, Ray CJ, Kirschner DE (2008) A methodology for performing global uncertainty and sensitivity analysis in systems biology. *J Theor Biol* 254:178–196.

[15] Minty JJ, et al. (2011) Evolution combined with genomic study elucidates genetic bases of isobutanol tolerance in *Escherichia coli*. *Microb Cell Fact* 10:18.

[16] Juhász T, Szengyel Z, Réczey K, Siika-Aho M, Viikari L (2005) Characterization of cellulases and hemicellulases produced by *Trichoderma reesei* on various carbon sources. *Process Biochem* 40:3519–3525.

[17] Elbing K, Brent R (2001) *Current protocols in molecular biology* (John Wiley & Sons, Inc.), Media preparation and bacteriological tools.

[18] Kovarova-Kovar K, Egli T (1998) Growth kinetics of suspended microbial cells: from single-substrate-controlled growth to mixed-substrate kinetics. *Microbiol Mol Biol Rev* 62:646–666.

[19] Mashego MR, van Gulik WM, Vinke JL, Heijnen JJ (2003) Critical evaluation of sampling techniques for residual glucose determination in carbon-limited chemostat culture of *Saccharomyces cerevisiae*. *Biotechnol Bioeng* 83:395–899.

[20] Argyros DA, et al. (2011) High ethanol titers from cellulose by using metabolically engineered thermophilic, anaerobic microbes. *Appl Environ Microbiol* 77:8288–8294.

[21] Simonian MH, Smith JA (2001) *Current protocols in molecular biology* (John Wiley & Sons, Inc.), Spectrophotometric and colorimetric determination of protein concentration.

[22] Kaur J, Chadha BS, Kumar BA, Ghatora SK, Saini HS (2007) Purification and characterization of β-glucosidase from *Melanocarpus sp*. MTCC 3922. *Electron J Biotechnol* 10:2

[23] Xiao Z, Storms R, Tsang A (2005) Microplate-based carboxymethylcellulose assay for endoglucanase activity. *Anal Biochem* 342:176–178.

[24] Dashtban M, Maki M, Leung KT, Mao C, Qin W (2010) Cellulase activities in biomass conversion: measurement methods and comparison. *Crit Rev Biotechnol* 30:302–309.

[25] Foster CE, Martin TM, Pauly M (2010) Comprehensive compositional analysis of plant cell walls (lignocellulosic biomass) part II: carbohydrates. *J Vis Exp* p e1837.

[26] Bonaccorsi ED, et al. (2006) Transcriptional response of the obligatory aerobe *Trichoderma reesei* to hypoxia and transient anoxia: implications for energy production and survival in the absence of oxygen. *Biochemistry* 45:3912–3924.

[27] Smith KM, Liao JC (2011) An evolutionary strategy for isobutanol production strain development in *Escherichia coli Metab Eng* 13:674–681.

[28] Herpoel-Gimbert I, et al. (2008) Comparative secretome analyses of two *Trichoderma reesei* RUT-C30 and CI847 hypersecretory strains. *Biotechnol Biofuels* 1:18.

[29] Zhang YHP, Lynd LR (2004) Toward an aggregated understanding of enzymatic hydrolysis of cellulose: noncomplexed cellulase systems. *Biotechnol Bioeng* 88:797–824.

[30] Pakula TM, Salonen K, Uusitalo J, Penttilä M (2005) The effect of specific growth rate on protein synthesis and secretion in the filamentous fungus *Trichoderma reesei*. *Microbiology* 151:135–143.

[31] Kubicek CP, Messner R, Gruber F, Mandels M, Kubicekpranz EM (1993) Triggering of cellulase biosynthesis by cellulose in *Trichoderma reesei* - involvement of a constitutive, sophorose-inducible, glucose-inhibited β-diglucoside permease. *J Biol Chem* 268:19364–19368.

[32] Huang CP, Westman D, Quirk K, Huang JP (1988) The removal of cadmium(II) from dilute aqueous-solutions by fungal adsorbent. *Water Sci and Technol* 20:369–376.

[33] Kurath SF, Bump DD (1965) Hydrodynamic friction coefficients for cellodextrins in water. *J Polym Sci, Part A* 3:1515–1526.

[34] Esterbauer H, Steiner W, Labudova I, Hermann A, Hayn M (1991) Production of *Trichoderma* cellulase in laboratory and pilot scale. *Bioresour Technol* 36:51–65.

[35] Bader J, Bellgardt KH, Schügerl K (1993) Modelling and simulation of the enzymatic hydrolysis of potato pulp by a complex enzyme mixture. *Chem Eng J Bioch Eng* 52:B13–B19.

[36] Baez A, Cho KM, Liao JC (2011) High-flux isobutanol production using engineered *Escherichia coli*: a bioreactor study with in situ product removal. *Appl Microbiol Biotechnol* 90:1681–1690.

[37] Lejeune R, Nielsen J, Baron GV (1995) Influence of pH on the morphology of *Trichoderma reesei* QM9414 in submerged culture. *Biotechnol Lett* 17:341–344.